

Targeting Low-Thrust Earth-Moon Transfer Trajectories with Ballistic Capture



Lam Tze King * ALIENA

Schedule

| | | | | |
|-----------|---------------------|--|-----------|--------------------|
| Section 0 | Preface | | | |
| Section 1 | Introduction | | | |
| Section 2 | Problem Formulation | | Section 4 | Results |
| Section 3 | Methodology | | Section 5 | Example Trajectory |
| | | | Section 6 | Discussion |
| | | | Section 7 | Bibliography |

0.1 – Log of Revisions

| Rev. Ver. & Date | Rev. Descr. |
|---------------------|---|
| v0.1 10 NOV 20 | Initial document creation First internal presentation |
| v0.2 07 DEC 20 | ADDED new section “Case for theoretical studies” under “Discussion” ADDED new section “Overview of in-depth studies” under “Discussion” First external presentation to OSTin |
| v0.3 08 FEB 21 | EDITED formats EDITED phraseology throughout presentation without change to technical meaning ADDED new header “Preface” ADDED new slide to section “Exterior WSB Trajectories to the Moon” under “Existing trajectories” Second external presentation to DSO technical staff |
| v1.1 29 MAY 21 | REORDERED slide sequence CHANGED reference numbers to authors’ last names REDUCED emphasis on exterior WSB, shifting presentation focus to interior WSB and theoretical build-up to simulation Third external presentation for Open Space SG 2021 |

0.2 – Disclaimer

- ▶ This presentation ("the content") is provided only for educational and informational purposes. ALIENA Pte Ltd ("the company") attempts to ensure that the content is accurate and obtained from reliable sources but does not represent it to be error-free. The company may add, amend or remove any constituent of the content, and failure to timely post such changes to the content shall not be construed as a waiver of enforcement.
- ▶ The content is protected under Fair Dealing, Copyright Act Chapter 63 of the Singapore Statutes, where a certain amount of copying for legitimate purposes, such as research and education, is permissible so long as it is a "fair dealing".
- ▶ All rights reserved. No part of the content may be reproduced, transferred or copied without explicit written approval from the company.

1.1 – Patched Conics Transfer

- Influence of more massive central celestial object, is ignored when operating within an orbiting body's sphere of influence (SOI):

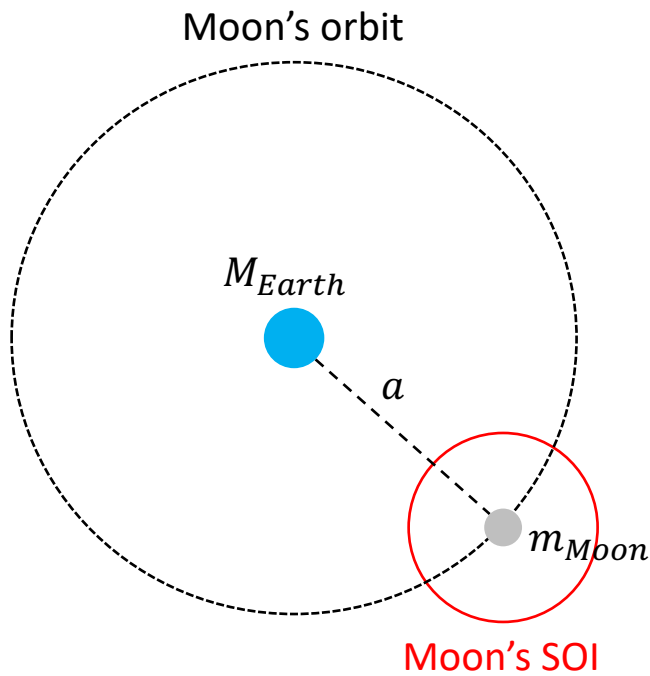


Figure 1: Moon's SOI with respect to Earth is ca. 66,000 km, ignoring the effects of the Sun. For reference, the Earth-Moon L_1 Lagrange point is located ca. 122,000 km from Earth.

$$r_{SOI} \approx a \left(\frac{m}{M} \right)^{0.4}$$

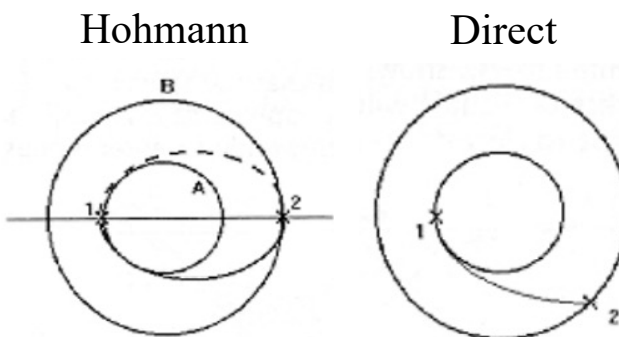


Figure 2: Illustrations of the Hohmann and direct and transfer trajectories.

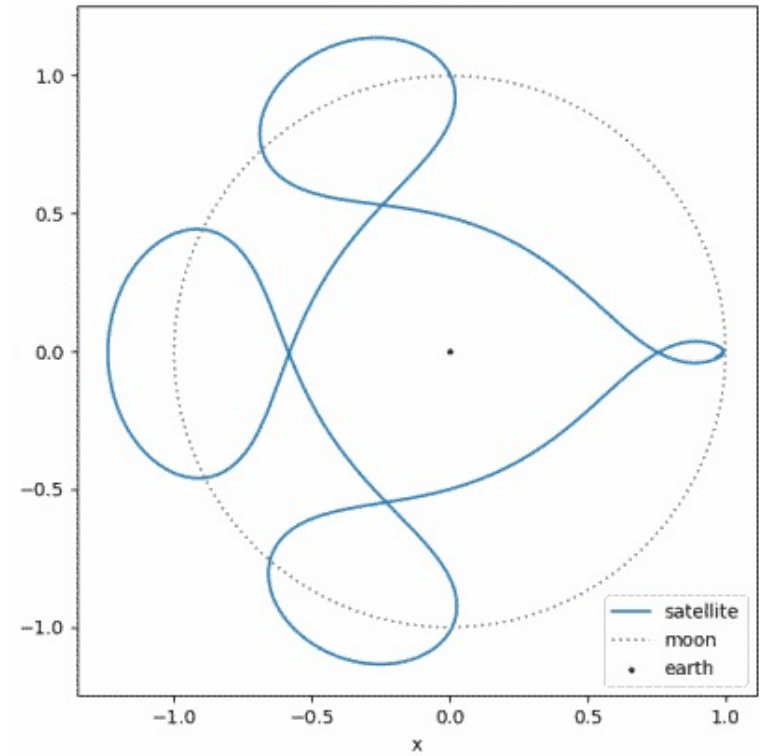
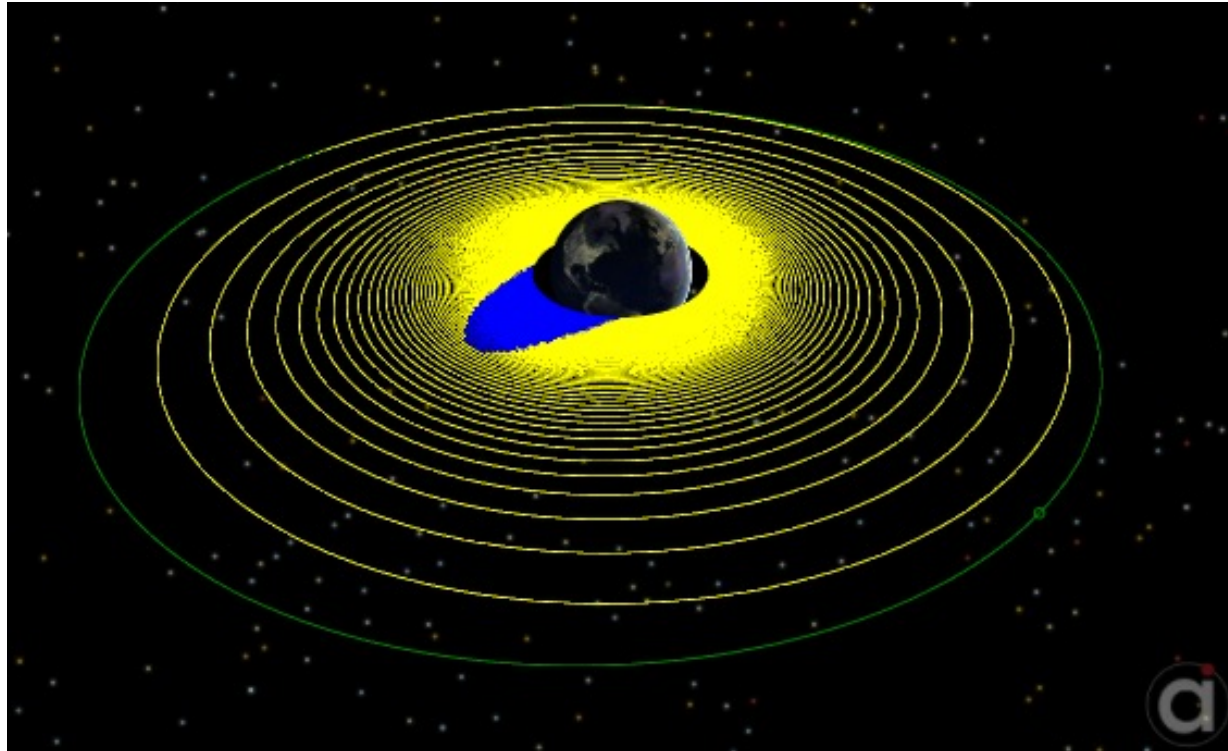


Figure 3: Apollo missions utilize Arenstorf orbits, which are stable periodic CPR3BP orbits with free return (Arenstorf 1963).

1.2 – Earth Spiral



Credit: https://ai-solutions.com/_help_Files/smp_elecspiraltogeo.png

Figure 4: Spiraling transfer orbit from LEO to GEO. Blue areas denotes times when the Spacecraft was in shadow.

1.3 – Ballistic Lunar Capture

- ▶ Permanent capture in the restricted three-body problem is impossible (Fesenkov 1946, Araujo 2008) without performing lunar insertion burn
- ▶ Temporal lunar capture without maneuvering possible by targeting the neck region near one of the Earth-Moon libration points (Conley 1968)

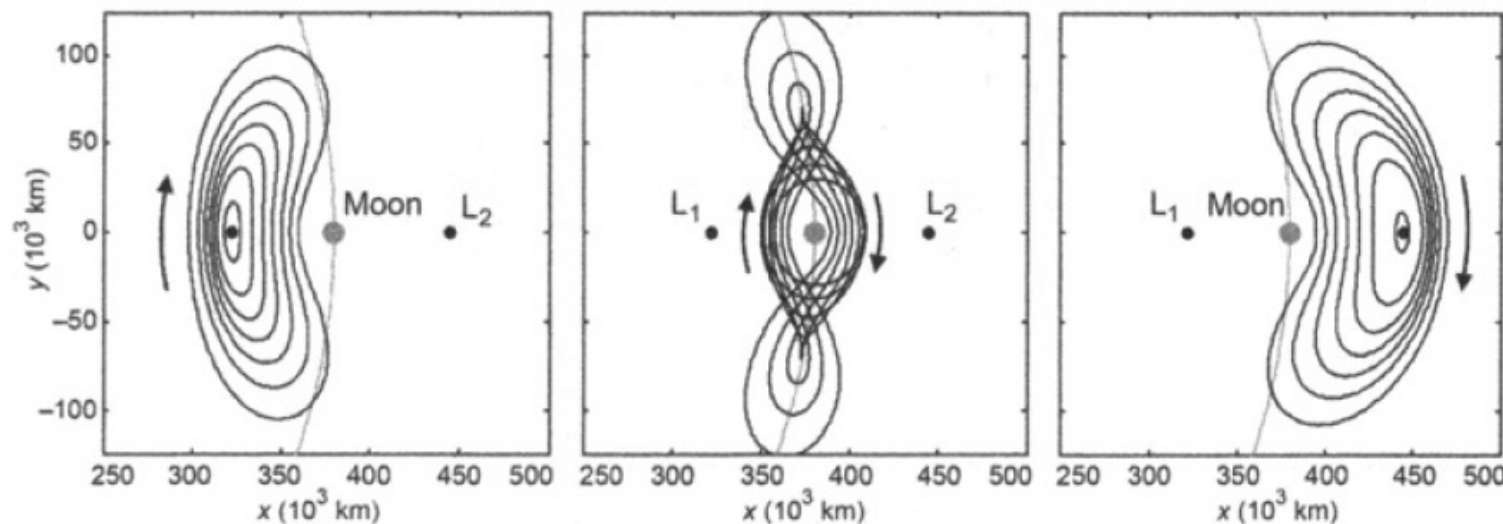


Figure 5: Several example orbits from three families of unstable periodic Earth-Moon three-body orbits, view from above in the Earth-Moon synodic reference frame. From left to right: Lyapunov orbits (L_1), distant prograde orbits, Lyapunov orbits (L_2). (Parker et al. 2014)

1.3 – Ballistic Lunar Capture

- Particle-secondary body characteristic energy (Yamakawa 1992):

$$C_3 = \|\mathbf{v}\|^2 - \frac{2\mu}{\|\mathbf{r}\|}$$

- ▷ Hyperbolic movement: $C_3 > 0$
- ▷ Elliptical movement: $C_3 < 0$ (temporary gravitational capture)

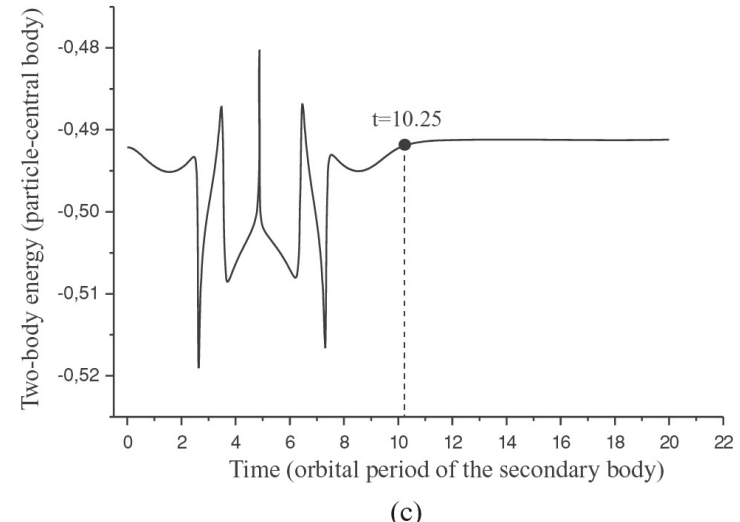
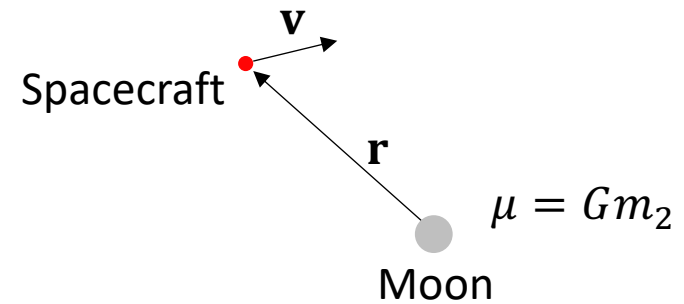
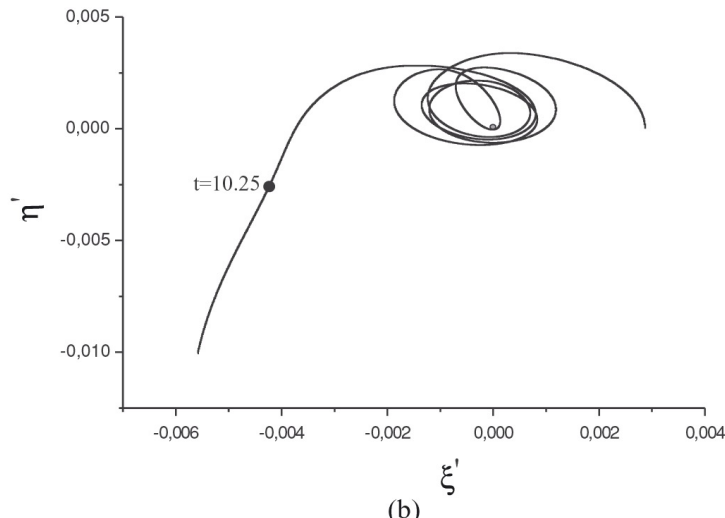
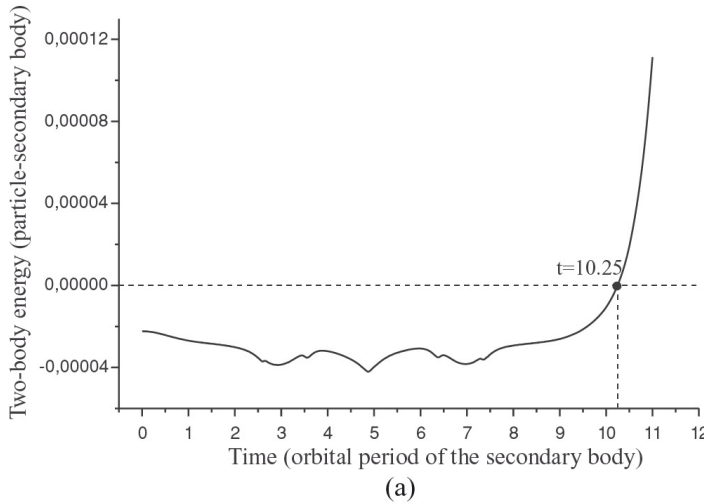


Figure 6: Particle with $v = 0.0050$, $r = 0.00287$ and $\mu_2 = \frac{m_2}{m_1+m_2} = 10^{-7}$. (a) Particle-secondary two-body problem energy; integration time equal to 11 orbital periods of secondary body. (b) Trajectory in a planetocentric inertial reference frame (centred at barycentre); integration time equal to 11 orbital periods of secondary body. (c) Particle-primary body energy; integration time equal to 20 orbital periods of secondary body. (Araujo et al. 2008)

1.4 – Restricted Three Body Problem

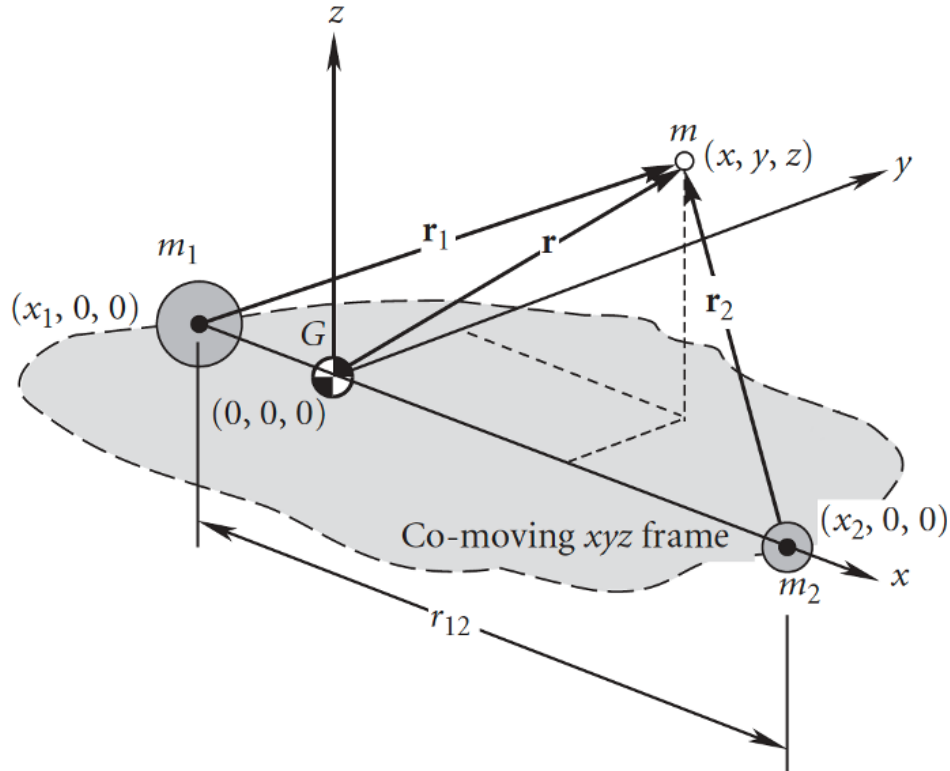


Figure 7: Primary bodies m_1 and m_2 in circular orbit around each other, plus secondary mass $m = 0$. Non-inertial, co-rotating frame of reference xyz with origin located at the barycentre of the two-body system. (Curtis 2004)

► Scalar equations of motion of secondary mass (Curtis 2004):

$$\ddot{x} - 2\Omega\dot{y} - \Omega^2 x = -\frac{\mu_1}{r_1^3}(x + \pi_2 r_{12}) - \frac{\mu_2}{r_2^3}(x - \pi_1 r_{12})$$

$$\ddot{y} + 2\Omega\dot{x} - \Omega^2 y = -\frac{\mu_1}{r_1^3}y - \frac{\mu_2}{r_2^3}y$$

$$\ddot{z} = -\frac{\mu_1}{r_1^3}z - \frac{\mu_2}{r_2^3}z$$

► Notations:

- ▷ Inertial angular velocity: $\boldsymbol{\Omega} = \Omega \hat{\mathbf{k}}$
- ▷ Dimensionless mass ratios: $\pi_1 = \frac{m_1}{m_1+m_2}$, $\pi_2 = \frac{m_2}{m_1+m_2}$
- ▷ Gravitational parameters: $\mu_1 = Gm_1$, $\mu_2 = Gm_2$

1.5 – Planar Restricted Three Body Problem

- Velocity in inertial and rotating frame related by:

$$\mathbf{v}_{int} = \mathbf{v}_{rot} + \boldsymbol{\omega} \times \mathbf{r}$$

- Consider secondary mass constrained to the plane $z = 0$:

$$\mathbf{v}_{int} = \begin{pmatrix} \dot{x} \\ \dot{y} \\ 0 \end{pmatrix} + \begin{pmatrix} 0 \\ 0 \\ \Omega \end{pmatrix} \times \begin{pmatrix} x \\ y \\ 0 \end{pmatrix} = (\dot{x} - y\Omega)\hat{i} + (\dot{y} + x\Omega)\hat{j}$$

- Lagrangian formulation for rotating frame: note explicit time independence

$$L = T - V$$

$$L = \frac{1}{2}[(\dot{x} - y\Omega)^2 + (\dot{y} + x\Omega)^2] + \frac{\mu_1}{r_1} + \frac{\mu_2}{r_2}$$

1.5 – Planar Restricted Three Body Problem

- Legendre transformation to Hamiltonian:

$$H(q_i, p_i, t) = \sum_i p_i \dot{q}_i - L(q, \dot{q}, t)$$

$$p_i = \frac{\partial L}{\partial \dot{q}_i}$$

- Conjugate momenta:

$$p_x = \dot{x} - y\Omega$$

$$p_y = \dot{y} + x\Omega$$

- Hamiltonian is explicitly independent of time (Noether's theorem implies temporal symmetry) and is thus conserved. This conserved value is the Jacobi integral, C :

$$H(x, y, p_x, p_y) = (p_x \dot{x} + p_y \dot{y}) - \frac{1}{2} [(\dot{x} - y\Omega)^2 + (\dot{y} + x\Omega)^2] - \frac{\mu_1}{r_1} - \frac{\mu_2}{r_2} = C$$

1.5 – Planar Restricted Three Body Problem

- For the PR3BP, C is the only conserved quantity and may be interpreted as the total energy of the secondary particle relative to the rotating frame:

$$H(x, y, p_x, p_y) = \frac{1}{2}(\dot{x}^2 + \dot{y}^2) - \frac{1}{2}\Omega^2(x^2 + y^2) - \frac{\mu_1}{r_1} - \frac{\mu_2}{r_2} = C$$

$$v^2 = \Omega^2(x^2 + y^2) + \frac{2\mu_1}{r_1} + \frac{2\mu_2}{r_2} + 2C$$

- By setting $v = 0$ for given value of C , we obtain curves of zero velocity from the equation above. These boundaries cannot be crossed by a secondary mass moving within an allowed region.

1.5 – Planar Restricted Three Body Problem

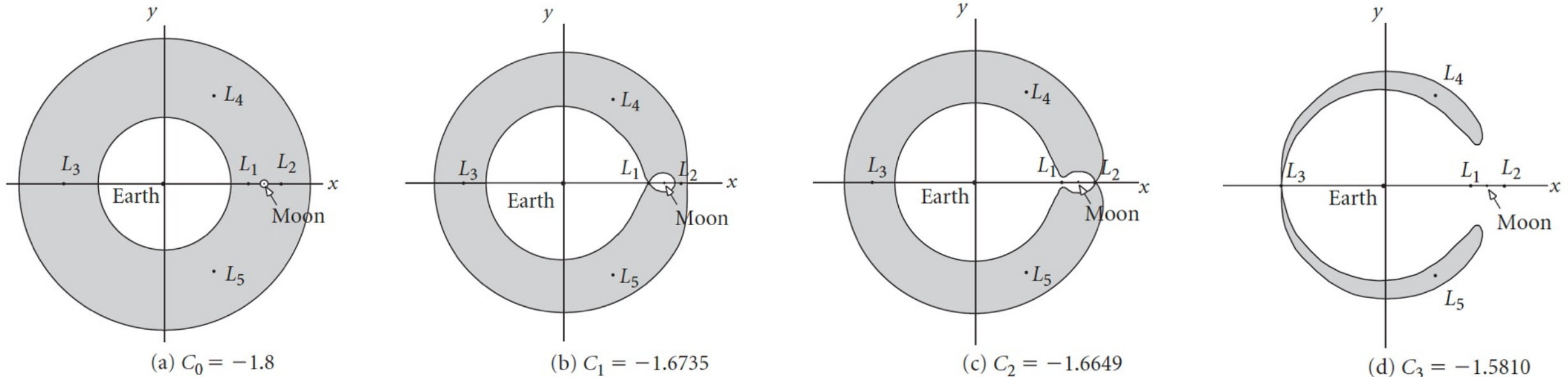
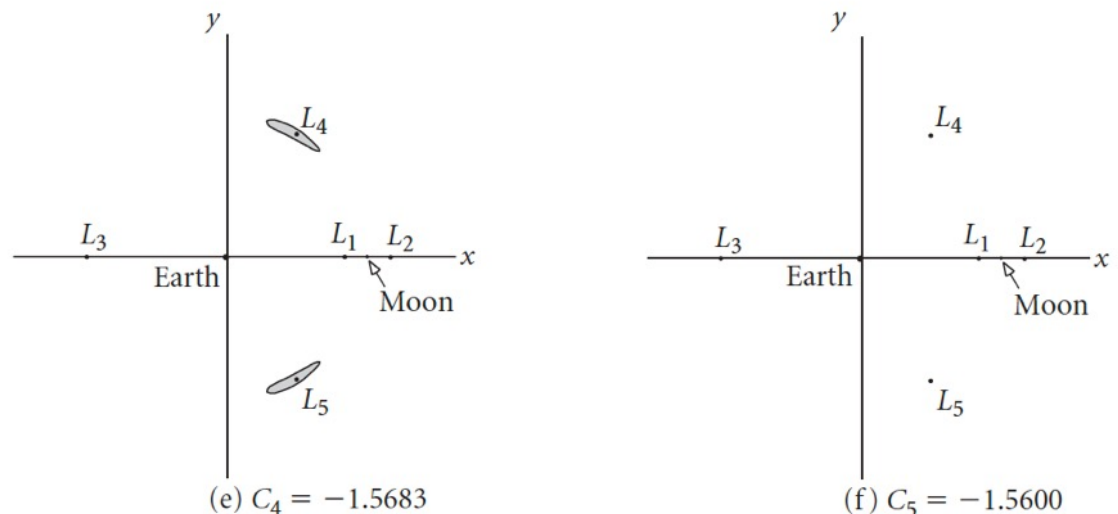
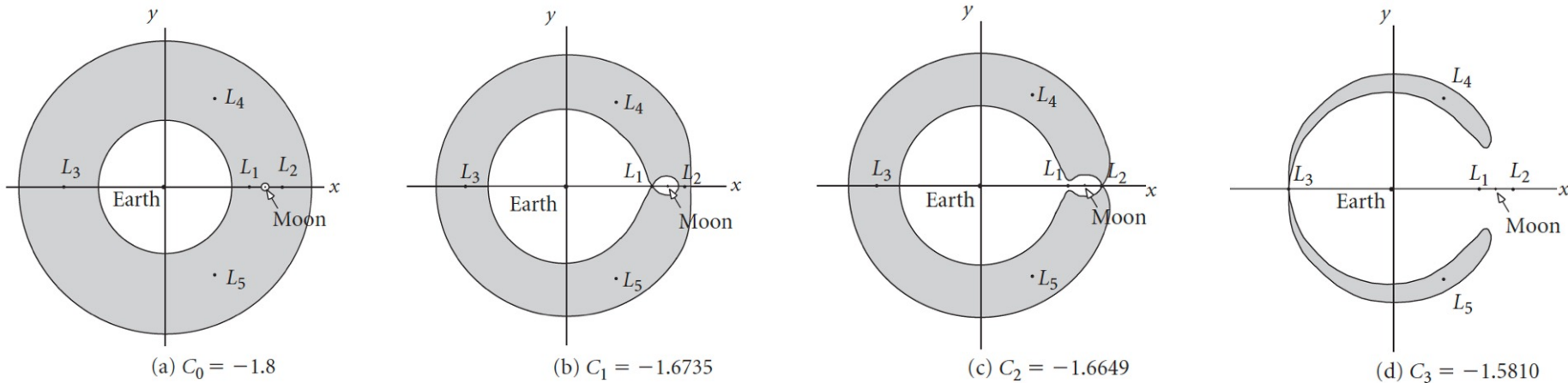


Figure 8: Forbidden regions (shaded) within the Earth-moon system for increasing values of Jacobi's constant (km^2/s^2). (Curtis 2004)



1.5 – Planar Restricted Three Body Problem



- ▶ Calculate burnout velocity of spacecraft at a point on the Earth-moon line with altitude of 200 km (parking orbit) for different values of Jacobi's constant:

$$C_0: v = 10.845 \text{ km/s}$$

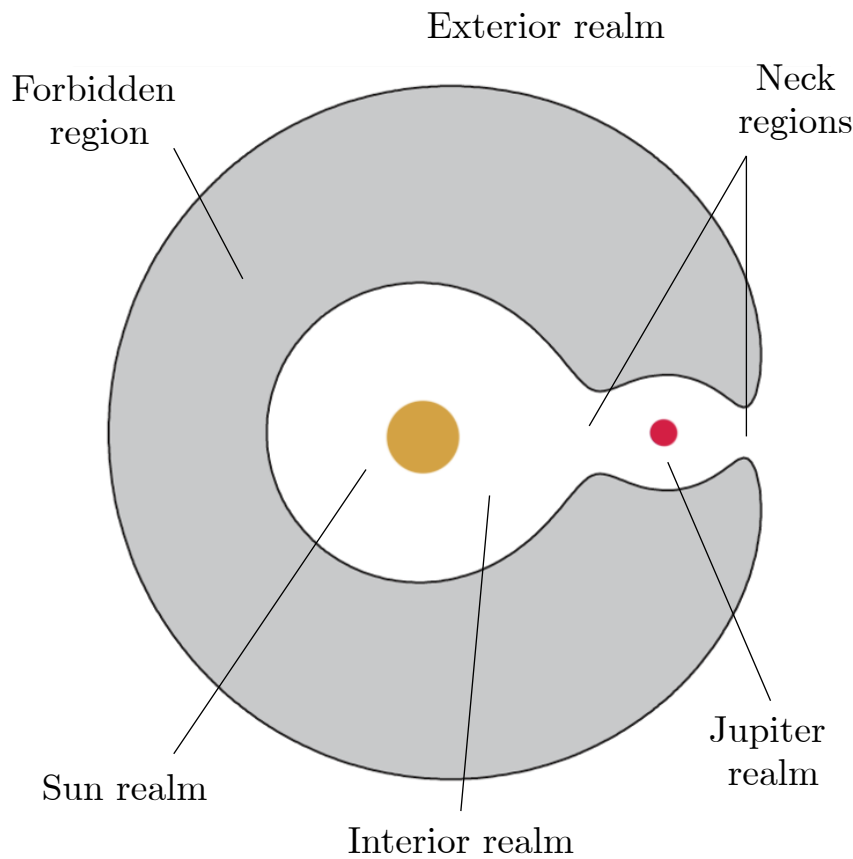
$$C_1: v = 10.857 \text{ km/s}$$

$$C_2: v = 10.858 \text{ km/s}$$

$$C_3: v = 10.866 \text{ km/s}$$



1.6 – Sun-Jupiter-Oterma System



- ▶ Comets moving in the vicinity of Jupiter do so mainly under the influence of Jupiter and the Sun
- ▶ Certain comets have been observed to make rapid transitions from **outside** of Jupiter's orbit to **inside** - **resonant transition**
- ▶ During transfer, the comet is captured temporarily by Jupiter

Figure 9: Level set showing Hill region with different areas labelled (Koon et al. 2007)

1.6 – Sun-Jupiter-Oterma system

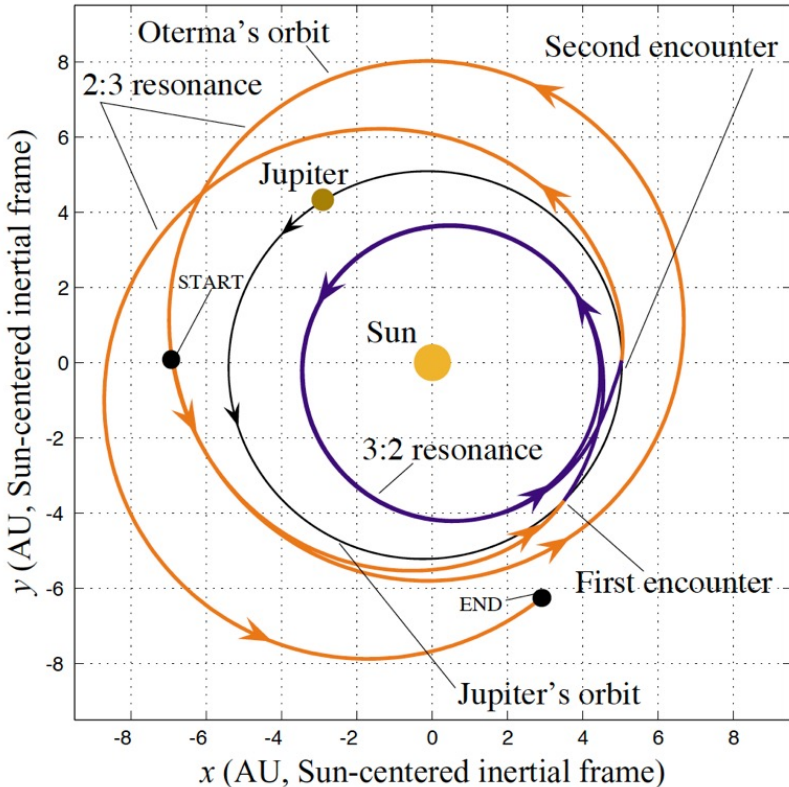


Figure 10: Orbit of comet Oterma from AD 1915-1980 in inertial frame. (Koon et al. 2007)

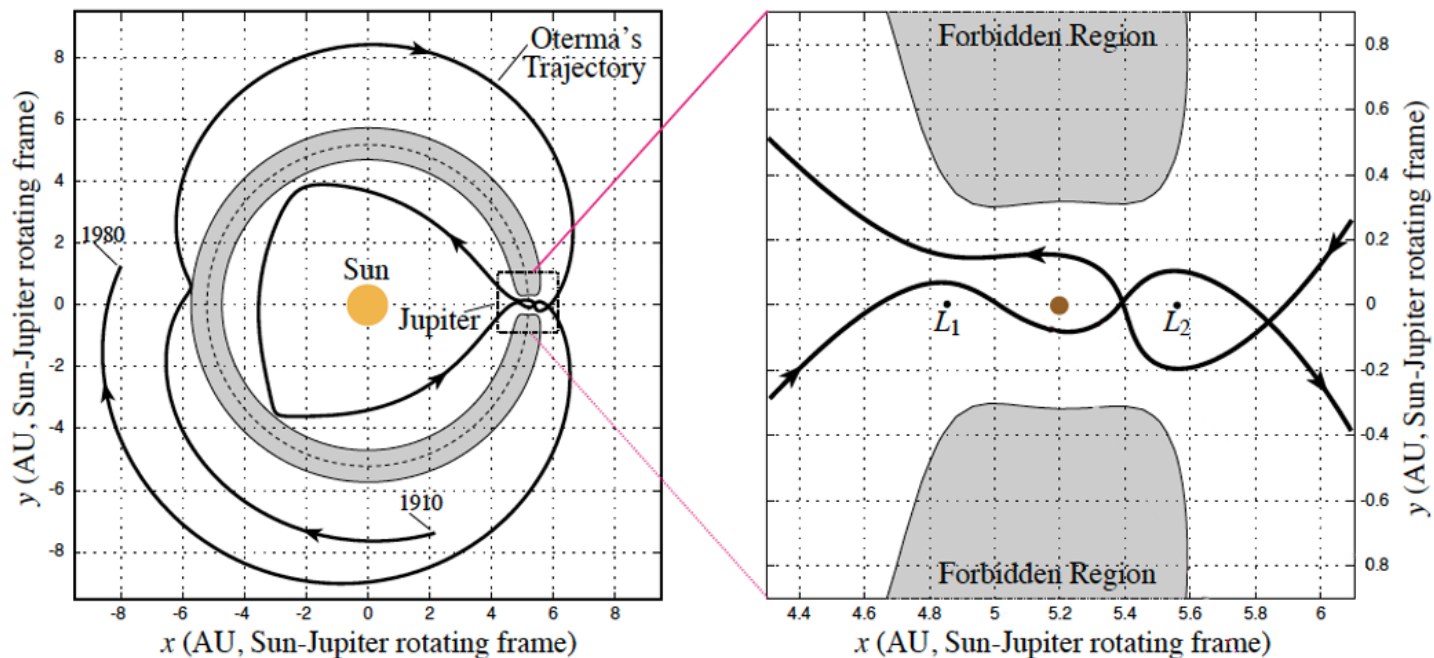


Figure 11: Orbit of comet Oterma from AD 1915-1980 in rotating frame, such that Jupiter appears to be still. (Koon et al. 2007)

1.7 – NASA's Lunar GAS Mission

- ▶ Overview of trajectory (Belbruno 1987):
 - ▷ Phase 1: Terran spiral outwards to point P
 - ▷ Phase 2: Capture orbit at point Q
 - ▷ Phase 3: Lunar spiral inwards
- ▶ Capture orbit constructed by back propagating from initial set of capture conditions

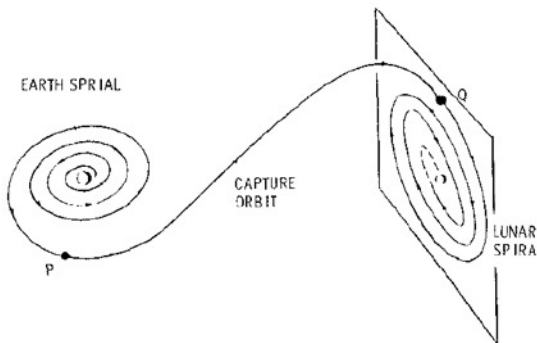
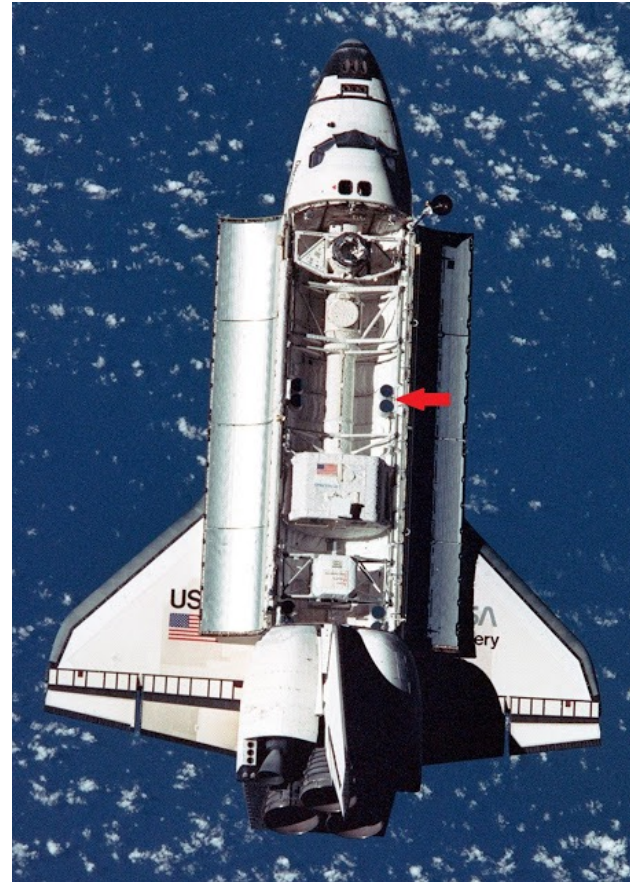


Figure 12: Earth-Moon low-thrust trajectory.



Credit: <http://shorturl.at/imxR7>

Figure 13: During STS-91, four pairs of GAS canisters were carried along the Shuttle's Payload Bay walls. The red arrow points to one pair.

1.8 – ESA's SMART-1 Mission

- Lunar mission study (Vasile et al. 2002) investigated lunar gravitational assists to minimize delta-v
 - ▷ Lunar resonance / perturbation: $\|\mathbf{r}\| < 160,000 \text{ km}$
 - ▷ Lunar flyby: $\|\mathbf{r}\| < 60,000 \text{ km}$
 - ▷ Lunar capture: $C_3 < 0$

| Phases | Trajectory |
|--------|---|
| 1 | Continuous thrusting to raise Earth orbit |
| 2 | Lunar perturbation to further raise Earth orbit |
| 3 | Lunar resonance |
| 4 | 1:1 resonant orbit / shaping orbit |
| 5 | Lunar capture (breaking manoeuvre) |
| 6 | Continuous thrusting to lower lunar orbit |

Table 3: SMART-1 Lunar Trajectory Optimization Stage Breakdown (Vasile et al. 2002).

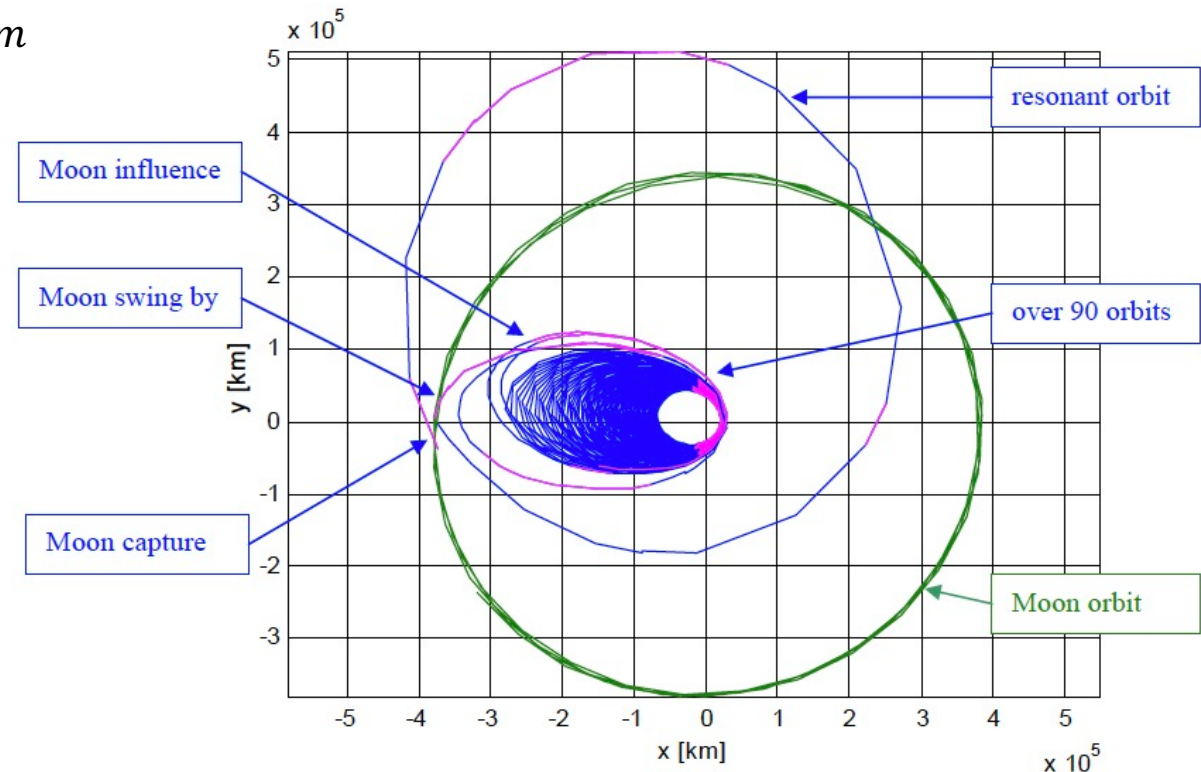


Figure 14: Complete SMART-1 trajectory in the Earth equatorial plane. Pink lines indicate thrust arcs (Vasile et al. 2002). Cruise phase is expected to last up to 18 months (Racca et al. 2002). Actual SMART-1 trajectory differs due to mission plan change (Rathsman et al. 2005).

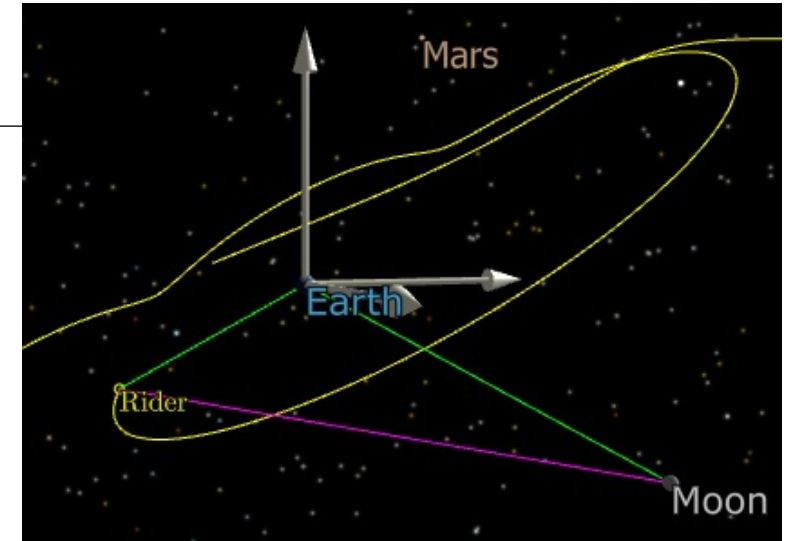
2.1 – Problem Statement

- ▶ Find transfer trajectory that:
 - ▷ Maximizes lunar orbit dwell time before ejection (quasi-stability)
 - ▷ Minimizes semi-major axis of departing stable high Earth orbit
 - ▷ Minimizes transfer delta-v (ballistic transfer)

3.1 – Conventions

► Color use:

- ▷ Spacecraft: yellow (coast arcs), red (burn arcs)
- ▷ Earth to Moon, Earth to Rider vector: lime green
- ▷ Moon to Rider vector: magenta



► Osculating Keplerian state parameters:

$$\{A : e : I : \text{RAAN} : \omega : \theta\} \quad [\text{Apoapsis} : \text{Periapsis}]$$

► Inertial Reference Frames:

- ▷ Earth-centered: J2000
- ▷ Moon-centered: Moon Principal Axis - Inertial at J2000

► Units:

- ▷ Period: hour
- ▷ Distance: kilometer
- ▷ Angle: degree

► Time:

$$t_n, n \in \mathbb{Z}$$

$$\dots \rightarrow t_{-1} \rightarrow t_0 \rightarrow t_1 \rightarrow \dots$$

3.2 – Simulation Parameters

- ▶ Spacecraft:
 - ▷ Dry Mass: 75 kg
 - ▷ Nominal thrust: 16 mN
 - ▷ Propulsion power: 400 W
- ▶ Astrodynamics models: FreeFlyer
 - ▷ DE430: JPL planetary ephemeris
 - ▷ Jacchia Roberts: atmospheric model with Solar Radiation Pressure
 - ▷ IRI 2007: ionosphere model, electron density data file
 - ▷ EGM96: Earth gravity model (point masses for Moon and the Sun);
J2 perturbation enabled
 - ▷ Runge Kutta 8(9): numerical integrator



3.3 – Initial Conditions (IC)

► Osculating Lunar Keplerian Parameters:

- ▷ Apogee = 60,000 km
- ▷ Perigee = 7000 km
- ▷ RAAN = 0
- ▷ ω = 180
- ▷ TA = 180
- ▷ I = 50

Fixed

Vary

► Backward propagation:

- ▷ Seek stable high Earth orbit
- ▷ Investigate presence of further lunar encounters
- ▷ Minimize Terran semi-major axis



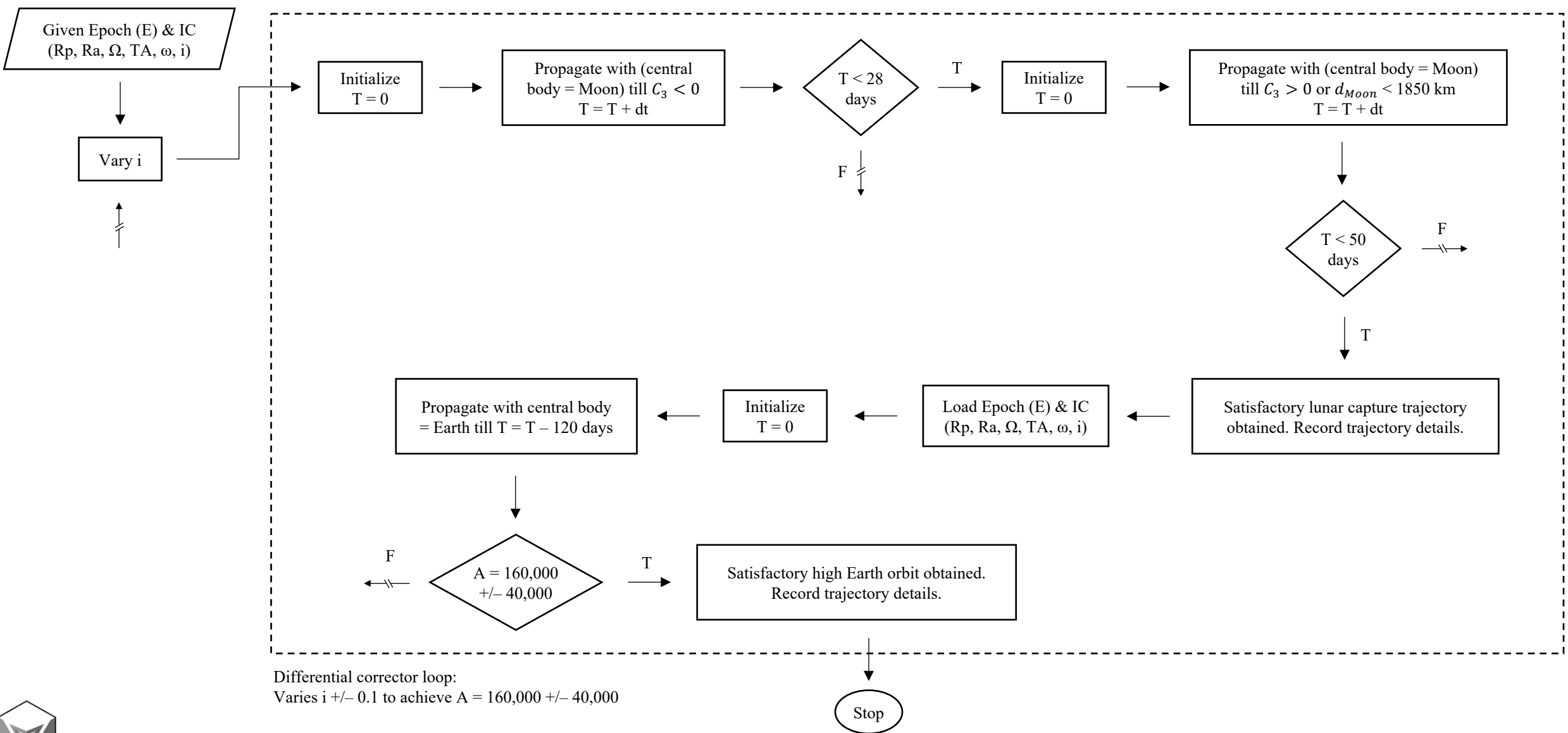
► Forward propagation:

- ▷ Investigation longevity of quasi-stable lunar orbit

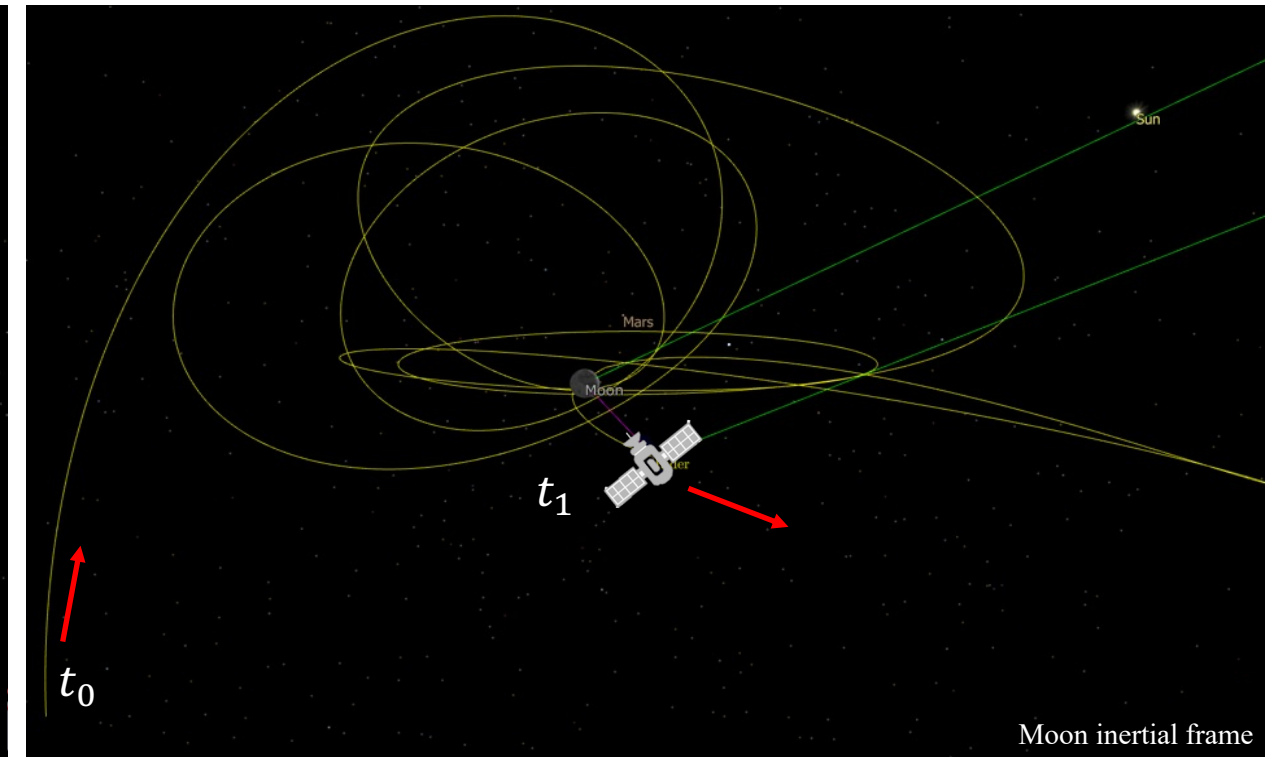
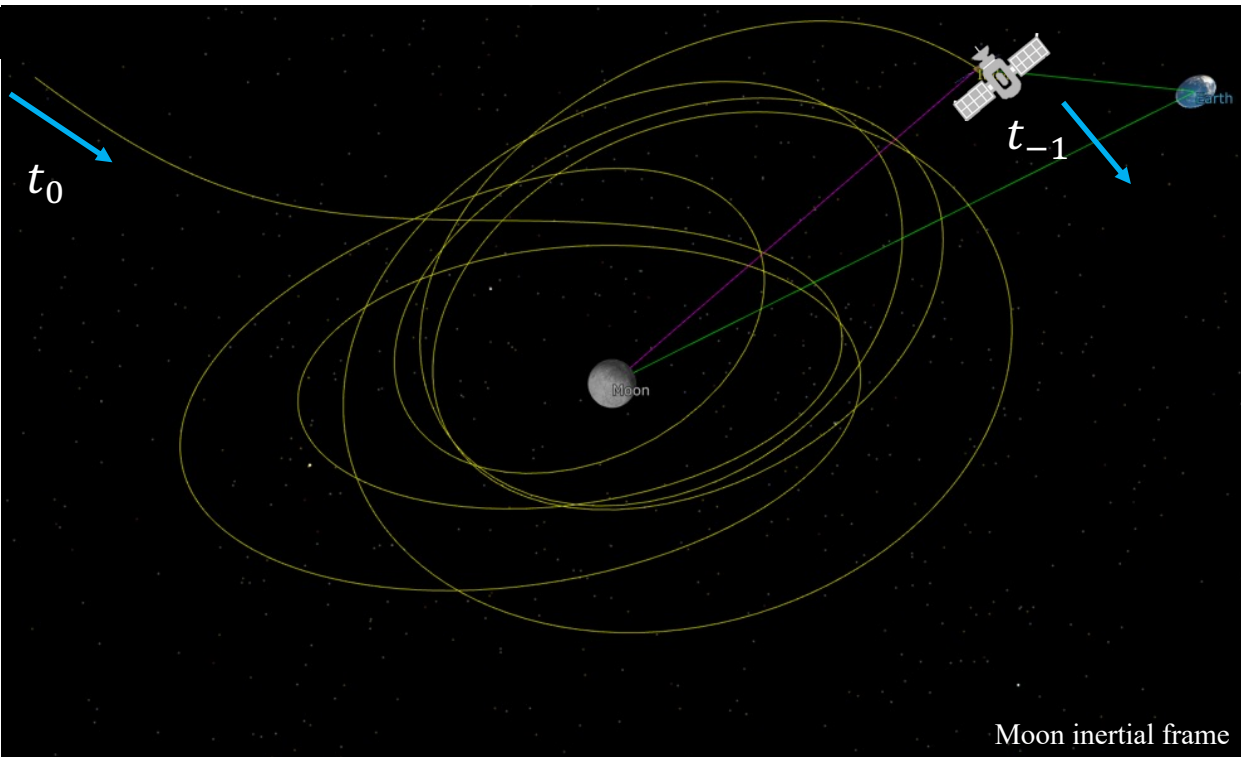


Epoch = 30885.609421296
Jul 29 2025 02:36:57.000 UTC

3.3 – Computation Process



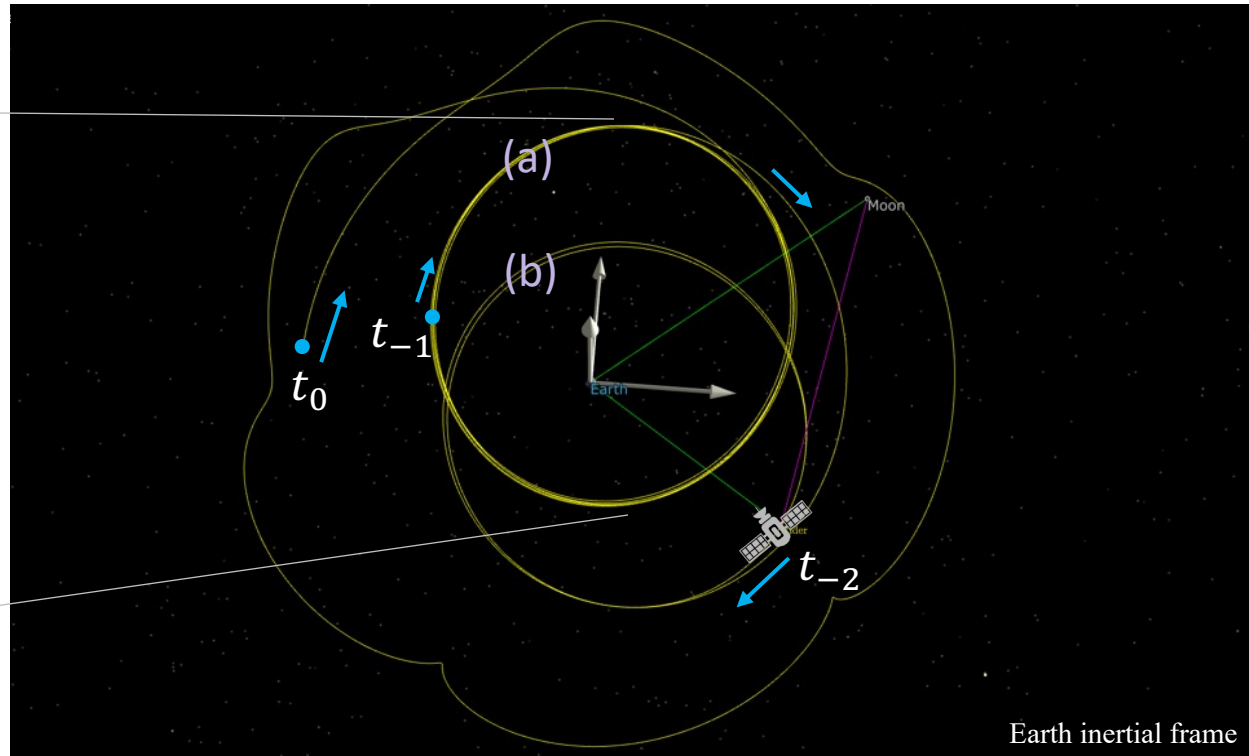
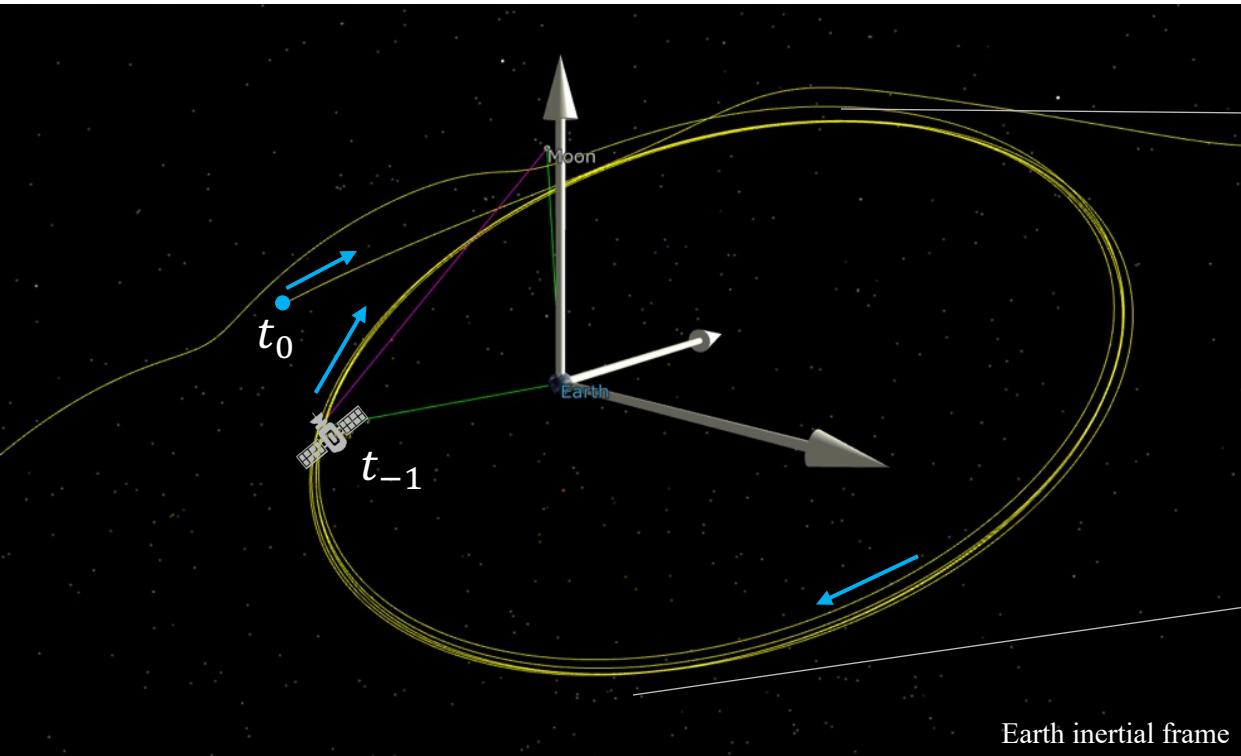
4.1 – Random Shooting



- ▶ Lunar ejection to Earth after 36 days (t_{-1}): 23 Jun 25
- ▶ Lunar proximity, closest approach of 7083 km: 13 Jul 25
- ▶ Lunar crash (t_1) after 33 days: 1193 km on 31 Aug 25
- ▶ Quasi-stability longevity: 69 days



4.1 – Random Shooting



- ▶ Stable high Earth orbit
- ▶ Osculating Terran Keplerian parameters: 18 Jun 25

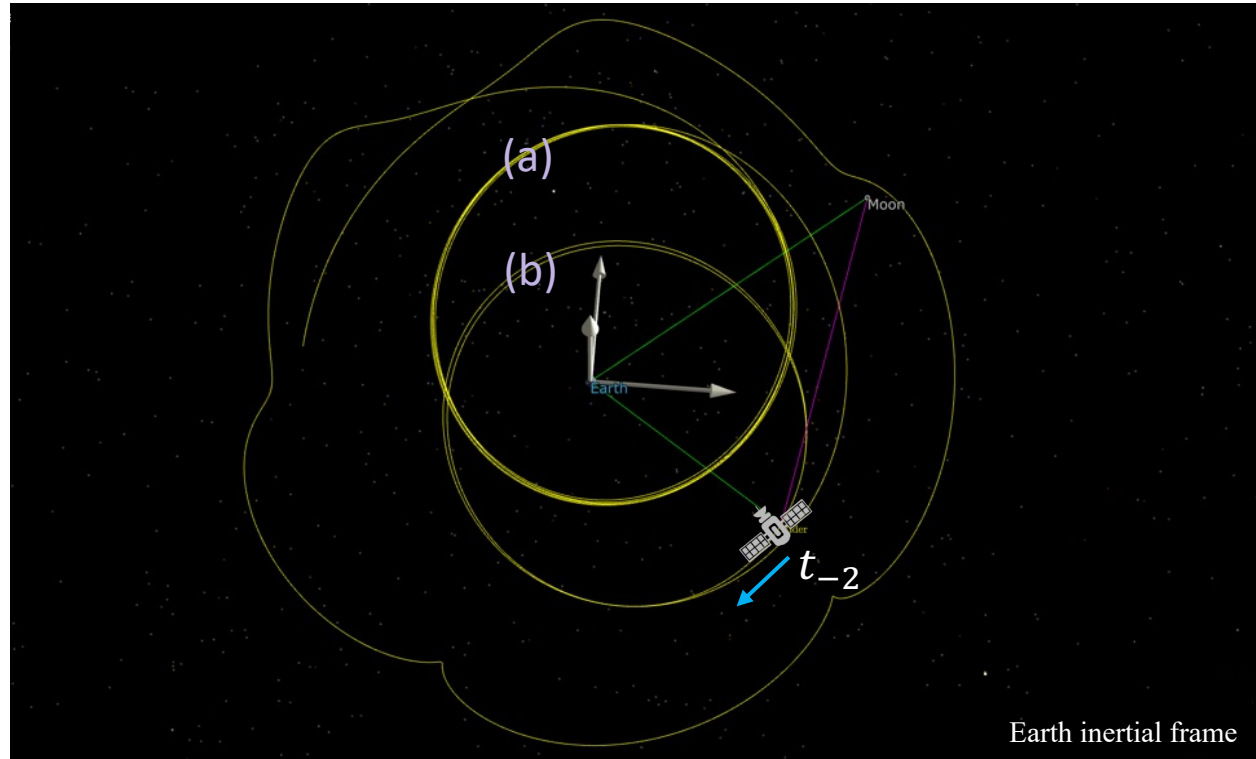
{**211 147** : 0.31171 : **32.59995** : 1.64609 : 252.4657 : 335.08952}

[**276 963** : 145 330]

- ▶ First Lunar resonance: 26 Apr 25, 70339 km
- ▶ Negative effect on Keplerian parameters: 31 Mar 25

{**213 995** : 0.35094 : 29.77864 : 7.44951 : 125.06112 : 195.45478}

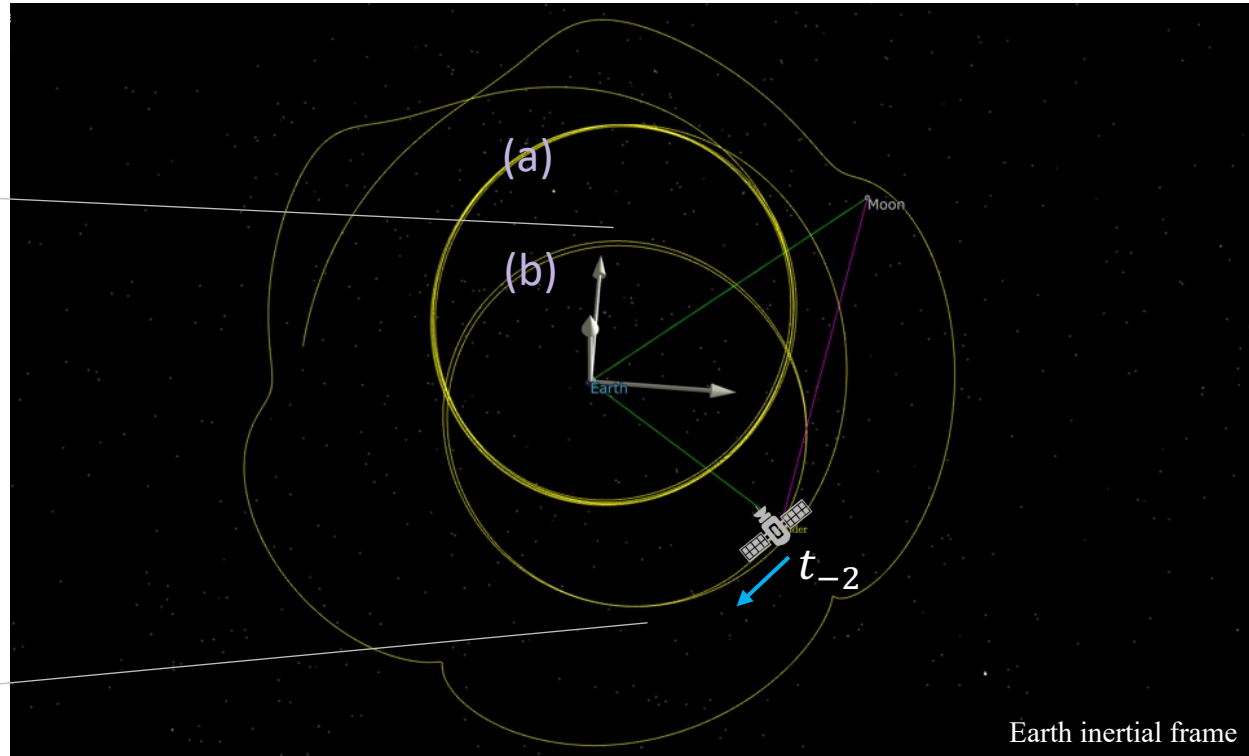
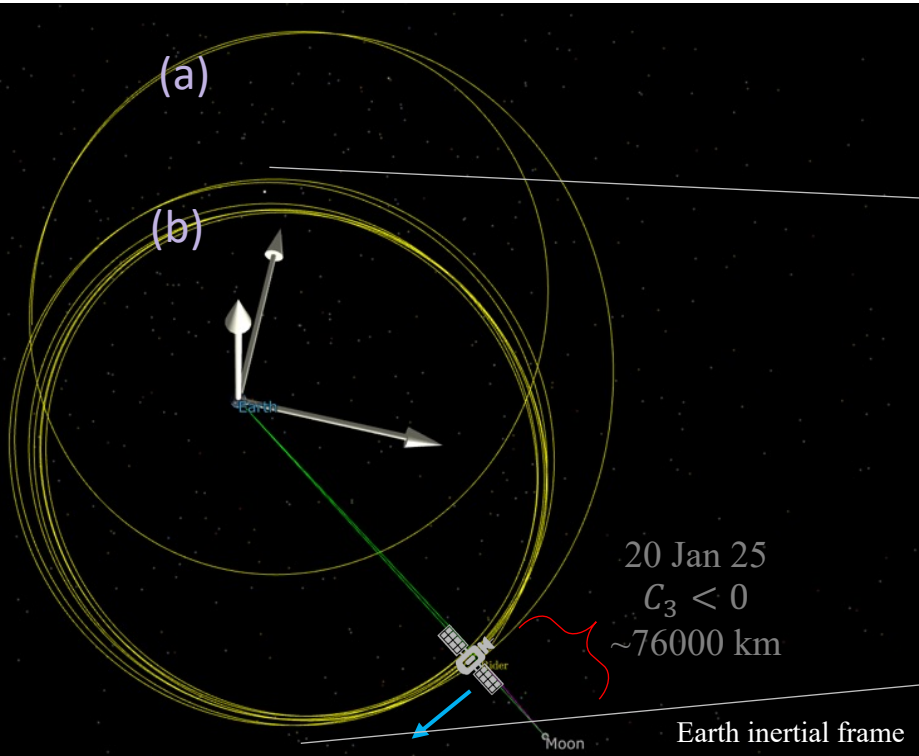
4.1 – Random Shooting



- ▶ Compare Moon and Spacecraft period at $t_{-2} = 5 : 2$
 - ▷ To first approximation, subsequent lunar encounter in ca. 54 days (05 Feb 25)



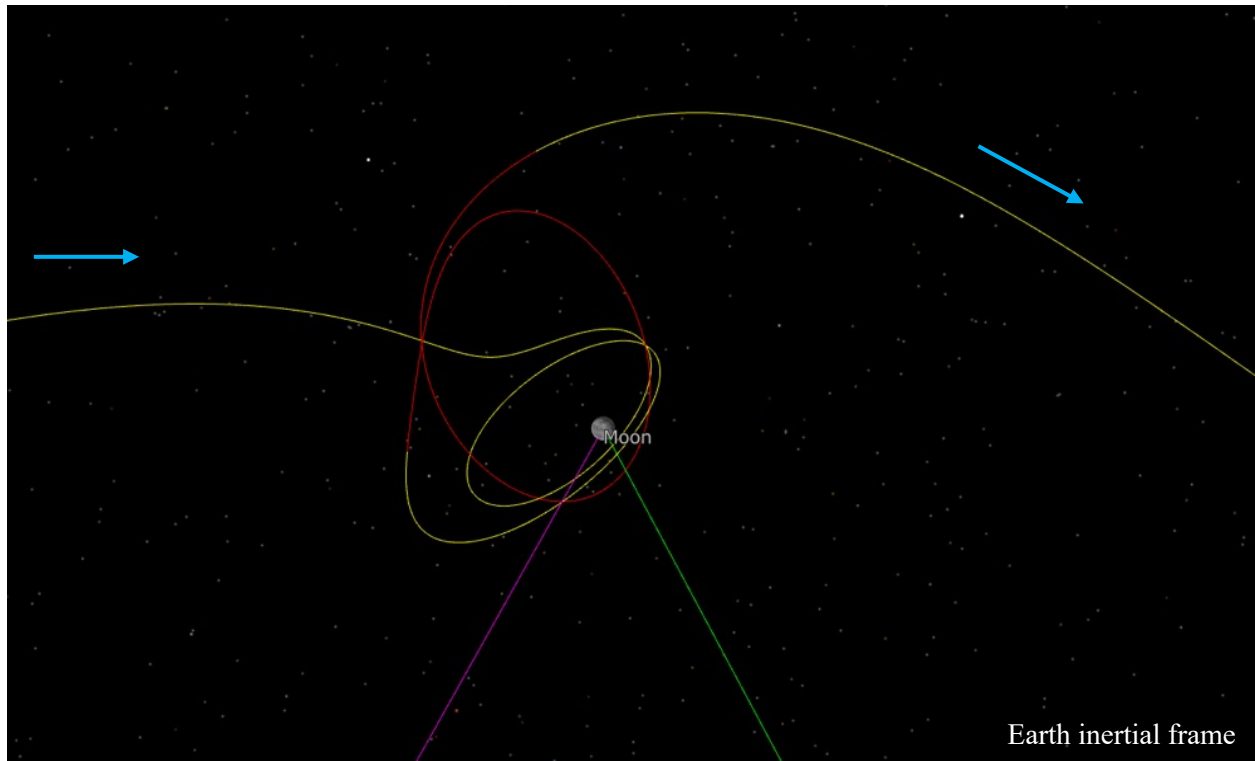
4.1 – Random Shooting



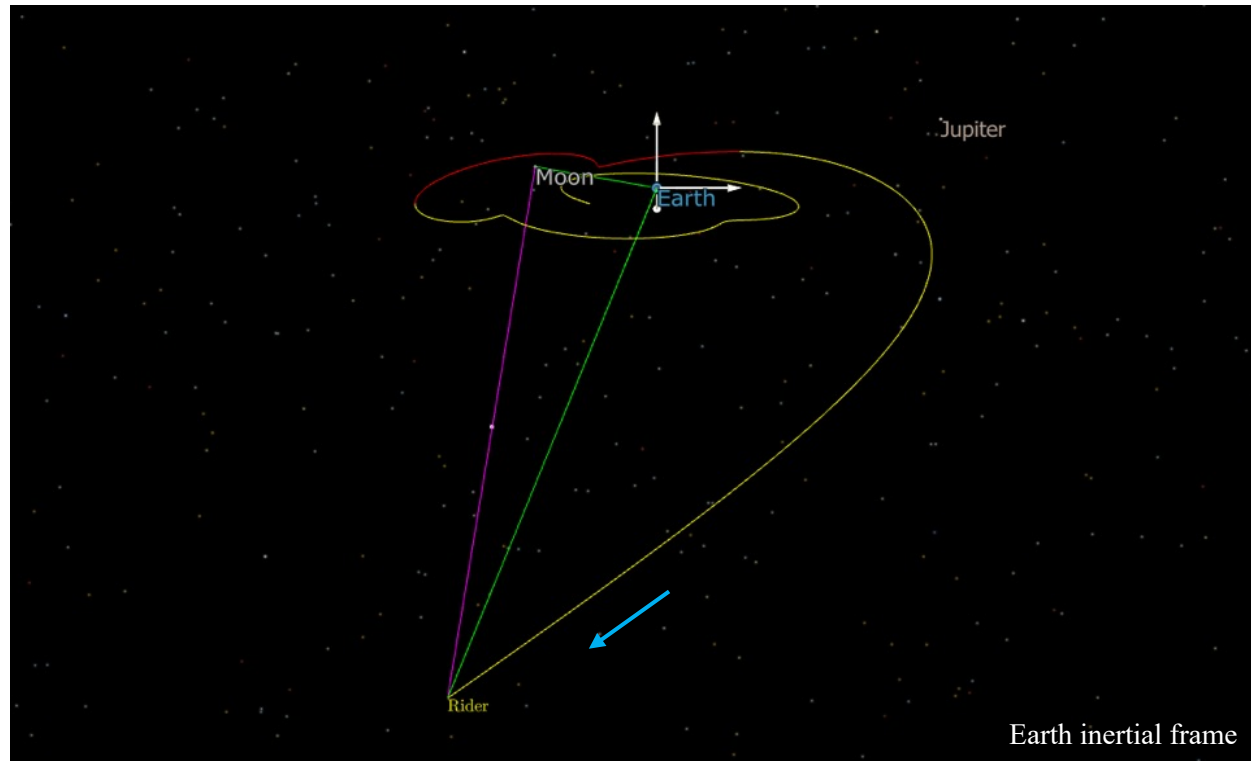
- ▶ Second Lunar resonance
- ▶ Compare Moon and Spacecraft period at $t_{-2} = 5 : 2$
 - ▷ To first approximation, subsequent lunar encounter in ca. 54 days (05 Feb 25)



4.1 – Random Shooting



Earth inertial frame



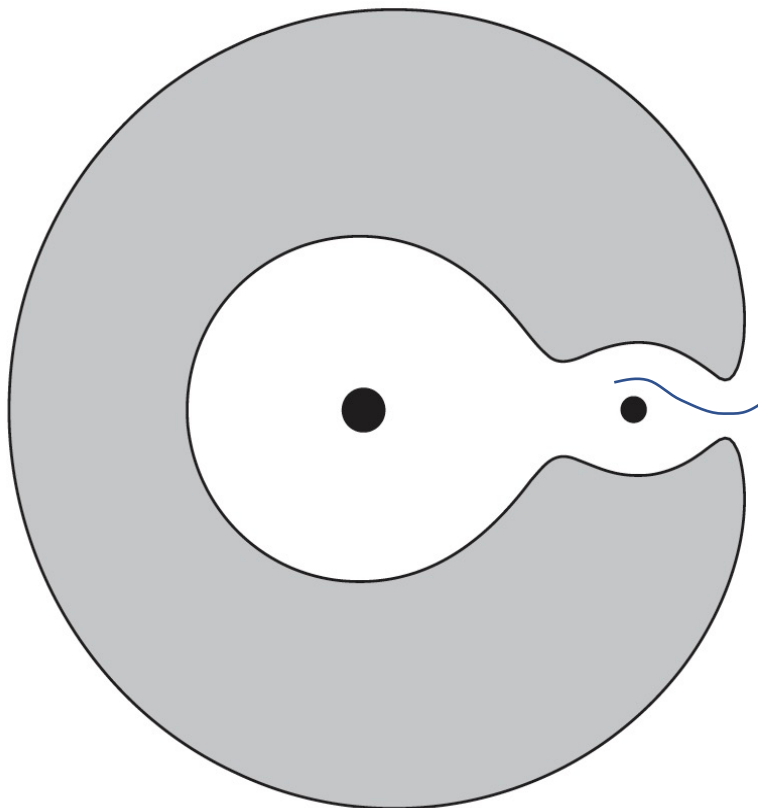
Earth inertial frame

► Red lines indicate firing of thrusters

► Moon-Earth system escape



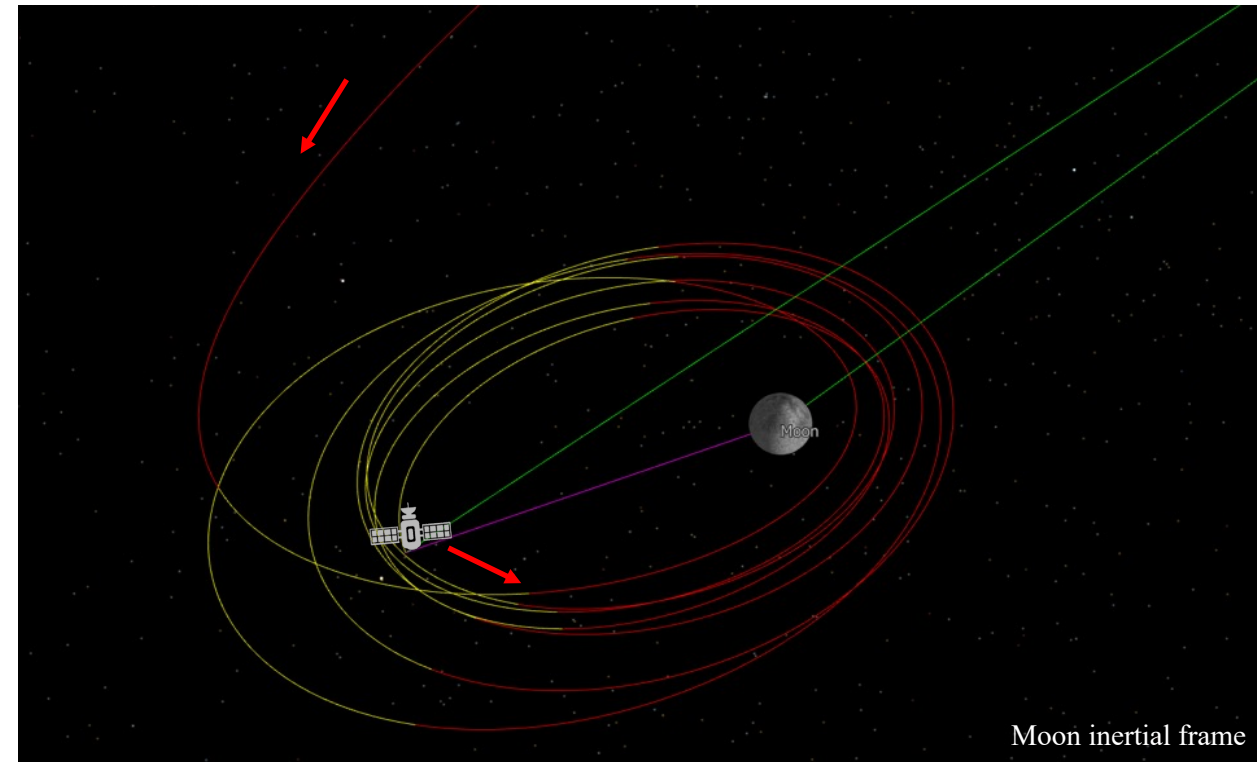
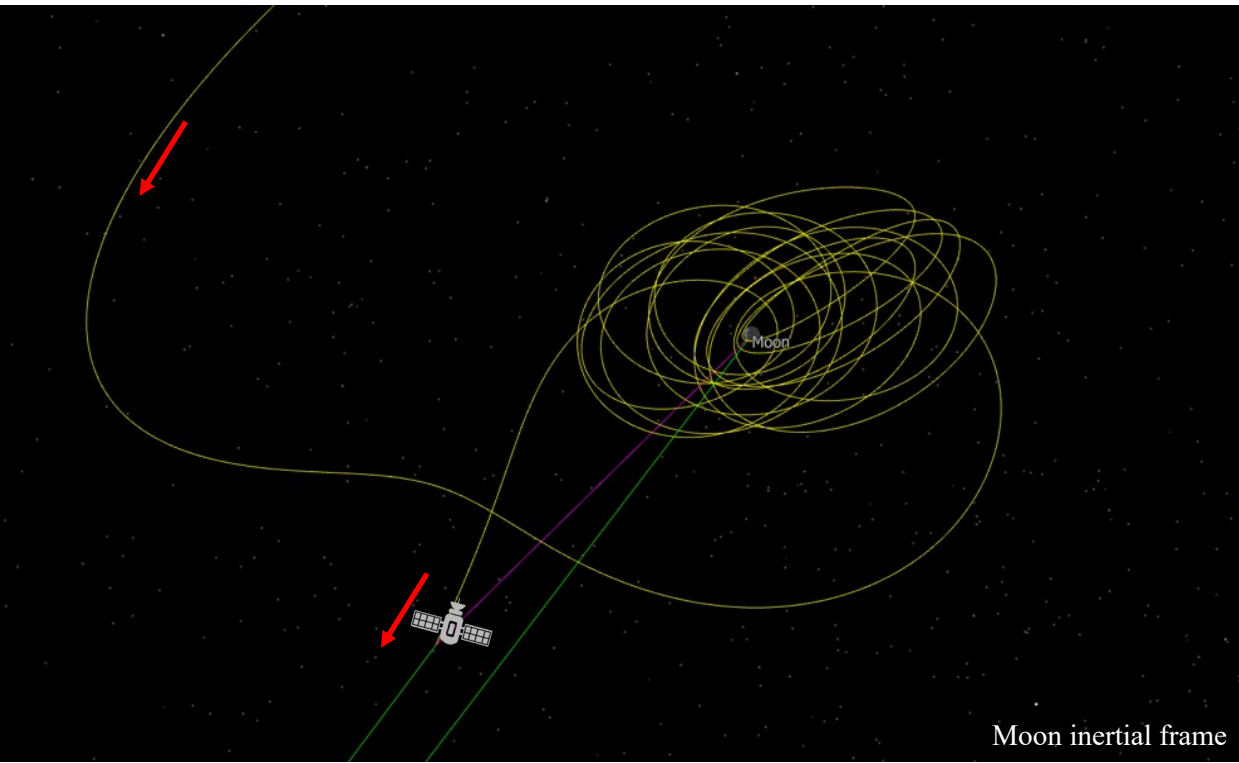
4.2 – Digression



Sun

New class of trajectories via **exterior Weak Stability Boundary**

4.3 – Converged Solution (Targetter)

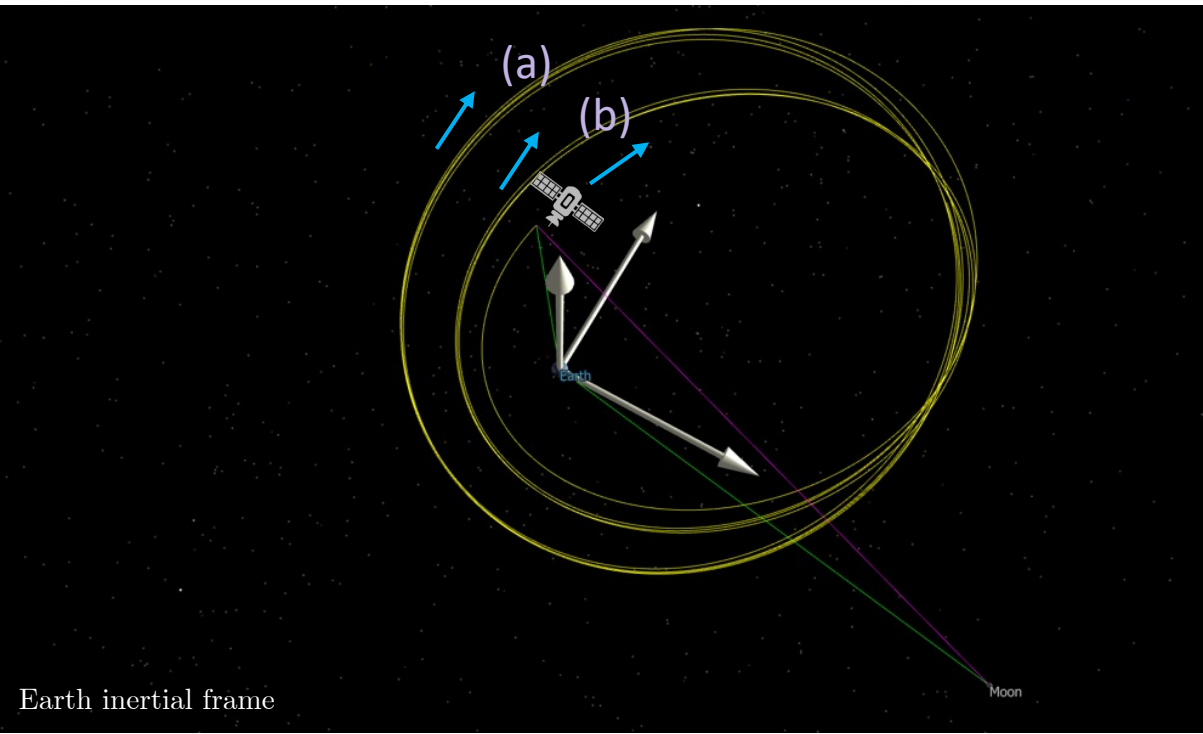


- ▶ Lunar capture ($C_3 < 0$): 20 Jul 2025, 02:54:27 UTC
- ▶ Quasi-stable Lunar orbit longevity: 84 days
- ▶ Closest approach: 2044 km at 2.14 km/s
- ▶ Lunar expulsion ($C_3 > 0$): 12 Oct 2025, 09:16:57 UTC

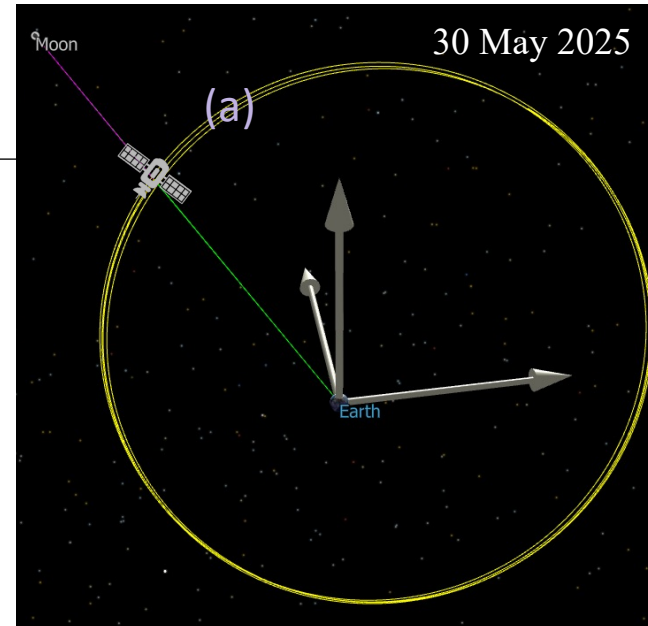
- ▶ Decelerating finite burns executed to stabilize orbit
- ▶ Priority is reducing apogee
- ▶ $\Delta v < 200$ m/s over 3 weeks



4.3 – Converged Solution (Targetter)

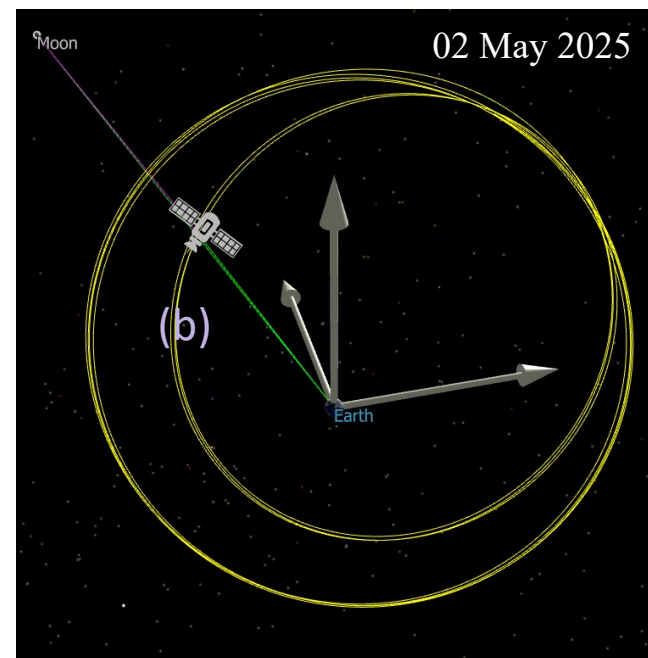


- First lunar resonance: 30 May 2025
 - ▷ Reduction on semi-major axis: 21 May 2025
- {**183 171** : 0.5485 : 30.949 : 228.8 : 248.2}; [**283 647** : **82 695**]
- Spacecraft period (216 hrs) : Moon period (663 hrs) = 1 : 3
 - ▷ Expect second lunar resonance: 03 May 2025



Orbital Plane Inclinations:

- Moon: 28.5 ± 0.2
- Rider: 31.0 ± 0.5



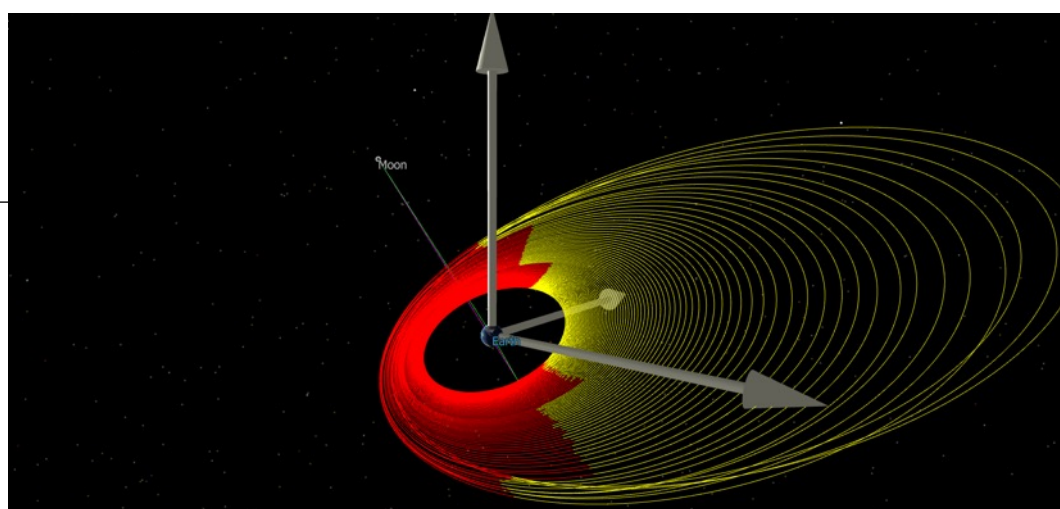
Further reduction in a :

- Apogee: 280 000
- Perigee: 61 730

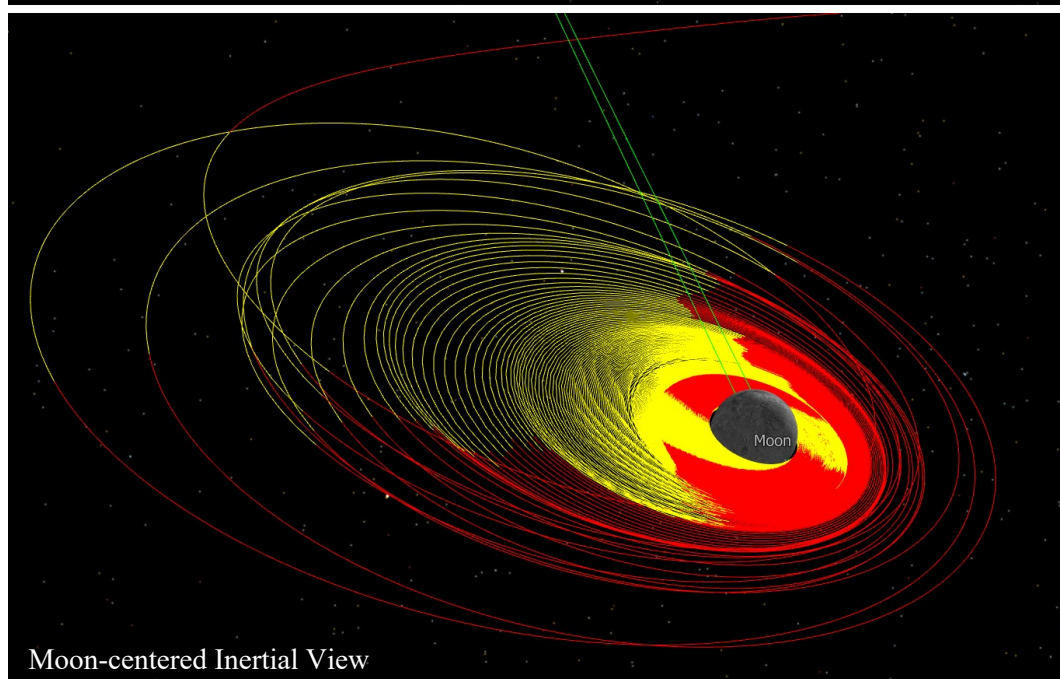


5.1 – Example Trajectory

| STATE | PHASE |
|---|---|
| α Geosynchronous Orbit | Phase 1: Spiral out of GSO, raise apogee |
| β First Lunar Resonance | Phase 2.1: Double Lunar resonance, no burns |
| γ Last Earth Perigee | Phase 2.2: Ballistic Lunar capture, no burns |
| δ Lunar Capture | Phase 3.1: Post capture burn, stability burns to lower apogee |
| ϵ High Elliptical Lunar Orbit | Phase 3.2: Circularize orbit |
| Ψ High Circular Lunar Orbit | Phase 3.3: Lower to LLO |
| Ω Low Lunar Orbit | |



Earth-centered Inertial View



Moon-centered Inertial View

5.1 – Example Trajectory

Table 4: Devil in the details.

Osculating Keplerian Parameters:
Orbit, Eccentricity, Inclination, [Period]

| Phase | Epoch (days) | Orbit Count | Burn Configuration (Thrust arc) | Fire Time (hours) | Fuel (kg) | Delta-V (m/s) | |
|------------|--------------|-------------|---|-------------------|-----------|---------------|--|
| 1 | 208 | 81 | -130 / +130 (40 orbits) -110 / +110 (31 orbits) -090 / +090 (10 orbits) | 1988 | 7.78 | 1327 | α 41 486 x 42 147, 0.008, 31.6 |
| 2.1 | 78 | 7 | Thruster OFF | 0 | 0 | 0 | β 81 790 x 285 409, 0.55, 31.1 |
| 2.2 | 5 | 0 | Thruster OFF | 0 | 0 | 0 | γ 131 069 x 278 901, 0.36, 30.2 |
| 3.1 | 69 | 70 | Continuous within Moon's SOI till Periapsis & Apoapsis < 45000 km | 130 | 0.51 | 91 | δ Rider-Moon Distance: 94 694 km Earth-Rider Distance: 276 155 km |
| 3.2 | 16 | 49 | -110 / +110 -110 / +110 till circularized orbit | 567 | 2.22 | 404 | ε 4442 x 6000, 0.15, 40.7, [9.4] Ψ 3970 x 3969, 0.000, 40.6, [6.2] |
| 3.3 | 57 | 463 | Continuous thrusting out of shadow, maintaining circular orbit with thrust arcs - 110 / +110 till periapsis < 1850 km | 186 | 0.73 | 135 | |
| Cumulative | 433 | 88, 582 | N.A. | 695 | 2.72 | 513 | Ω 1850 x 1860, 0.000, 40.5, [2.0] |
| | | | | 3566 | 13.96 | 2470 | |

Launch: NLT 22 Sep 24

Second lunar resonance:
30 May 25

Lunar capture:
19 Jul 25

High Circular Lunar Orbit:
12 Oct 25

> > >

M u s i c t o t h e m o o N

> > >

α GSO:
29 Sep 24

β First lunar resonance:
02 May 25

γ Last Earth Perigee:
14 Jul 25

ε High Elliptical Lunar Orbit:
26 Sep 25

Ω LLO: 08 Dec 25

6.1 – Comparisons with SMART-1

► Propulsion module:

- ▷ Power: 1225 W, 29 kg dry weight
- ▷ Nominal thrust: 68 mN
- ▷ Specific impulse: 1640 s
- ▷ Propellant: 82.5 kg Xe (4000 m/s)
- ▷ Storage: 150 bar, 49 L
- ▷ Thrust vector: 2-axis gimbal
- ▷ Initial acceleration: $2 \times 10^{-4} \text{ ms}^{-2}$

► Spacecraft:

- ▷ Mass: 367 kg, 284.5 kg (dry)
- ▷ Scientific payload: 19 kg, ca. 80 W
- ▷ Solar panels: 50.7 kg, 10 m^2 , 1850 W (BOL), 1615 W (EOL)
- ▷ Li-ion batteries: 5 x 130 Whr

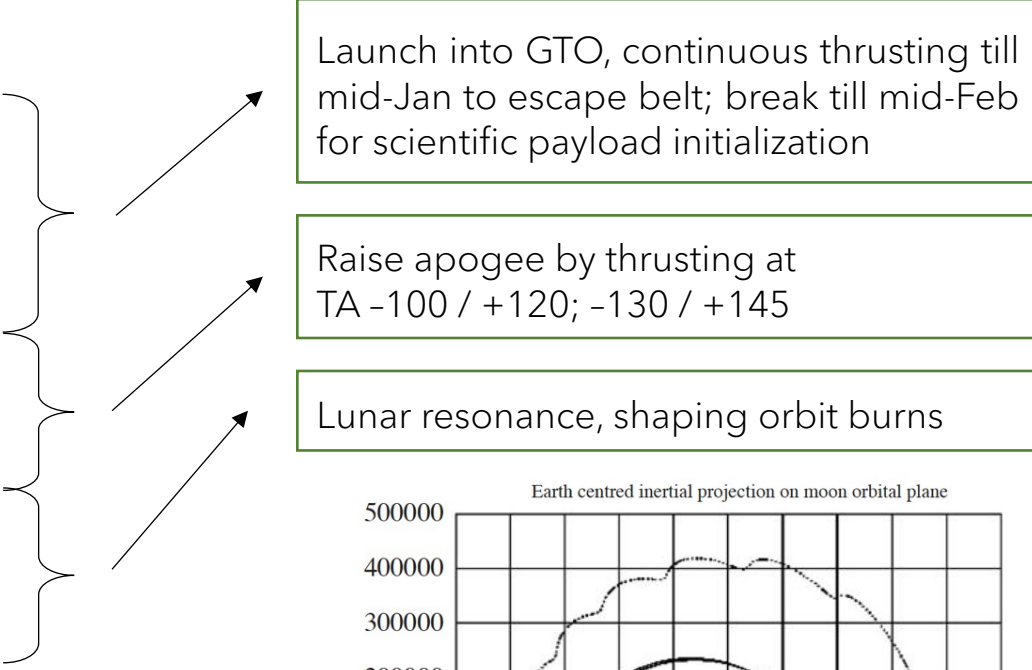


6.1 – Comparisons with SMART-1

| Epoch | Perigee (km) | Apogee (km) | I (°) | Period (hours) |
|------------------|---------------------|----------------|----------|-------------------|
| 27 Sep 03 | 7 035 | 42 223 | 6.9 | 10.7 |
| 19 Dec 03 | 13 390 | 49 369 | 6.8 | 15.4 |
| 19 Feb 04 | 20 691 | 65 869 | 6.9 | 24.9 |
| 19 Mar 04 | 20 683 | 66 916 | 7.0 | 25.3 |
| 25 Aug 04 | 37 791 | 240 824 | 6.9 | 144 |
| 19 Oct 04 | 69 959 | 292 632 | 12.5 | 213 |
| 24 Oct 04 | 179 718 | 305 214 | 20.6 | 330 |
| 02 Nov 04 | Last Terran perigee | | | |

Table 5: Summary of osculating geocentric orbital elements.

First lunar resonance: mid-Aug 04
 Second lunar resonance: 15 Sep 04
 Third lunar resonance: 12 Oct 04



| | |
|----------|---------------|
| ON Time: | 1700 hours |
| Delta-V: | 1300 m/s |
| ON Time: | 3200 hours |
| Delta-V: | 2500 m/s |
| ON Time: | 3648 hours |
| Delta-V: | 2737 m/s |
| Xe (kg): | 58.8 expended |

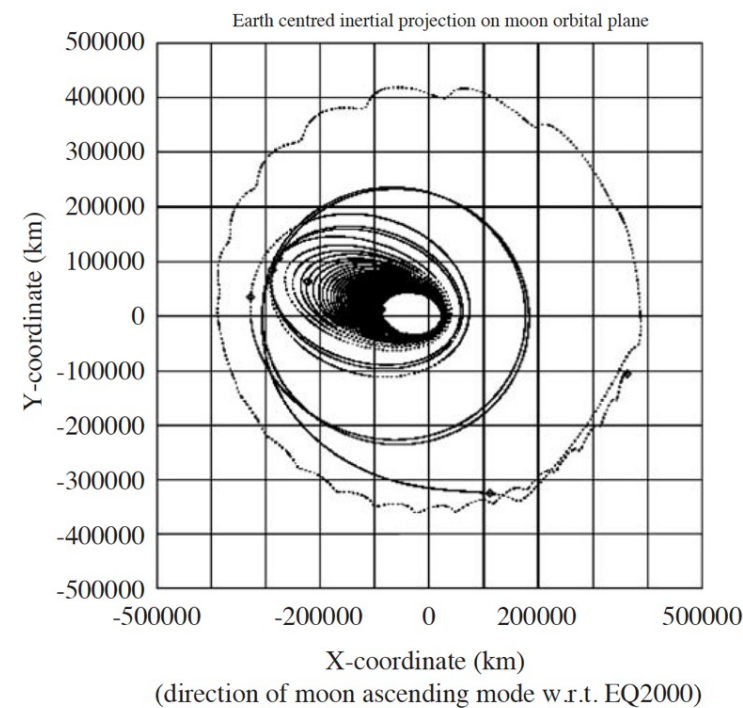
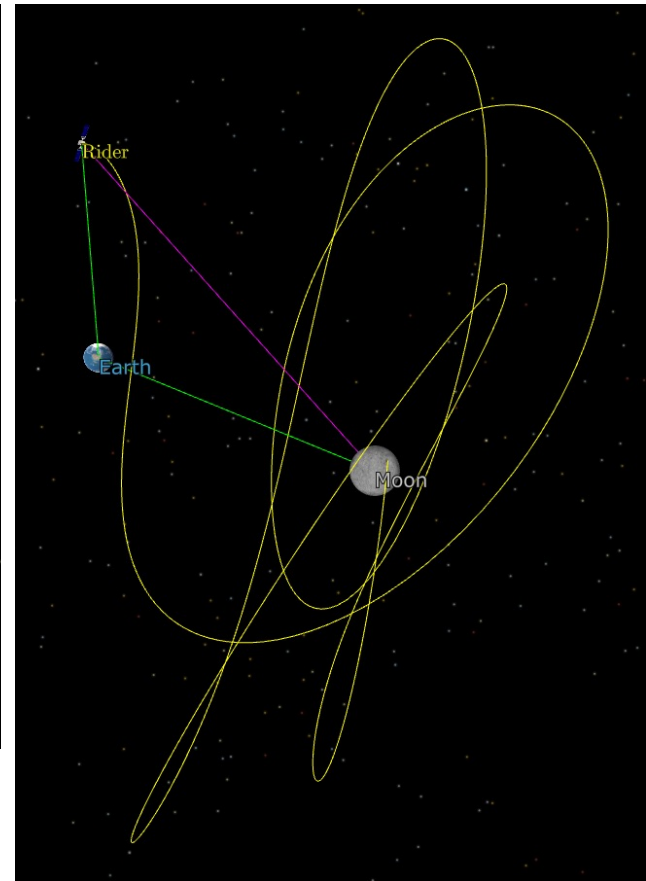
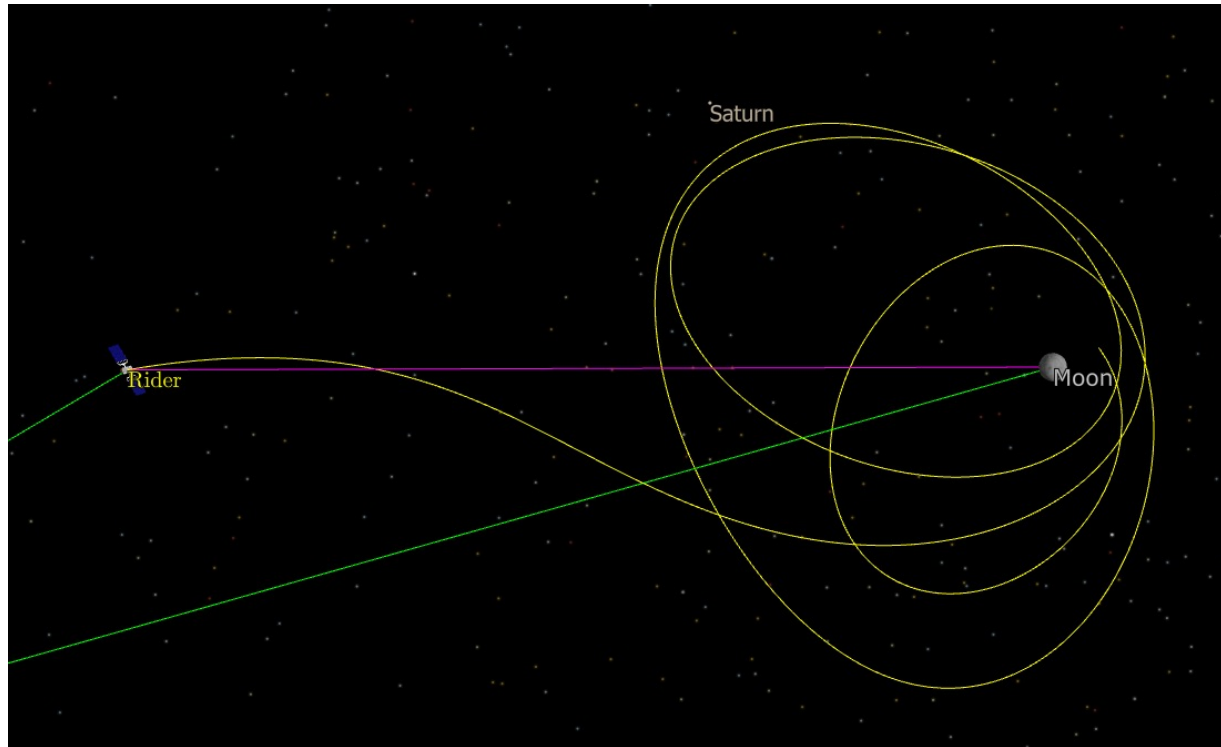


Figure 15: SMART-1 as-flown trajectory (Rathsman et al. 2005).

6.1 – Comparisons with SMART-1

- Osculating Selenocentric Orbital Elements (15 Nov 24, 17:47:38.700 UTC):

{29 955.958437 : 0.776195 : 81.077151 : 246.524941 : 308.011816 : 0} [53 207.630341 : 6 704.286533]



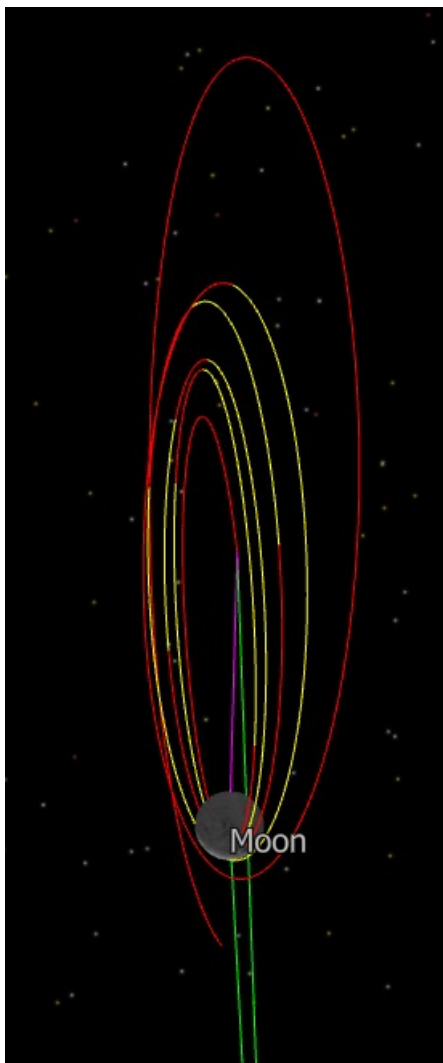
- Lunar expulsion within 24 days without braking maneuver

Planned Thruster Firings

| EP Start (Epoch) | EP End (Epoch) | Duration (sec) |
|--------------------|--------------------|----------------|
| 15 Nov 04 05:23:53 | 19 Nov 04 17:48:52 | 390 299 |
| 20 Nov 04 19:09:52 | 21 Nov 04 06:01:27 | 39 095 |
| 21 Nov 04 21:54:03 | 22 Nov 04 06:34:54 | 27 651 |
| 22 Nov 04 13:15:54 | 22 Nov 04 20:33:42 | 26 268 |
| 23 Nov 04 19:11:49 | 24 Nov 04 04:28:17 | 33 388 |
| 24 Nov 04 18:30:12 | - | 87 455 |



6.1 – Comparisons with SMART-1



| Summary of Osculating Selenocentric Orbital Elements | | | | |
|--|--------------|-------------|-------|----------------|
| Epoch | Perigee (km) | Apogee (km) | I (°) | Period (hours) |
| 15 Nov 04 | 6700 | 53 215 | 81 | 129 |
| 04 Dec 04 | 5 455 | 20 713 | 83 | 37.3 |
| 09 Jan 05 | 2 751 | 6 941 | 88 | 8.41 |
| 28 Feb 05 | 2 209 | 4 618 | 90 | 4.97 |

Key Events and Findings

- ▶ **11 Nov 04:** passed through L_1
- ▶ **15 Nov 04:** resumed thruster firing for 4.5 days to lower lunar orbit, estimated delta-v of 76 m/s, consuming ca. 1.6 kg of fuel at 4.1 mg/s mass flow, 1500 s I_{sp} ^[26]
- ▶ **Till mid-Jan 05:** lunar orbit lowering to orbit ID B0, consuming estimated 11.6 kg of fuel, ca. delta-v 570 m/s
- ▶ **B0 to B3:** 10.5 kg, delta-v 530 m/s
- ▶ **Total lunar delta-v:** ca. 1.2 km/s

| Orbit ID | Apocentre altitude (km) | Pericentre altitude (km) | Orbital period (hr) | Eclipse duration (hr) | Transfer time (days) | Propellant required (kg) |
|----------|-------------------------|--------------------------|---------------------|-----------------------|----------------------|--------------------------|
| B0 | 10,000 | 300 | 14.25 | 1.43 | — | — |
| B1 | 6000 | 300 | 8.52 | 1.11 | 16.5 | 4.6 |
| B2 | 4000 | 300 | 6.04 | 1.03 | 28.7 | 8.4 |
| B3 | 3000 | 300 | 4.92 | 1.01 | 36.8 | 10.5 |

Table 6: Main orbit characteristics of the operational lunar orbits (Racca et al. 2002)

6.2 – Moving Forward

Local optimization

- ▶ Utilizing FreeFlyer optimization engine - support for Nlopt, Ipopt
- ▶ Evaluation loop: initial ranged state variables → perform analysis → update constraints
→ optimize objective function with variables and weights



Local fine-tuning

- ▶ Enhance simulation realism and fidelity - building a better model
- ▶ Incorporate phase and plane change burns to achieve desired orbit
- ▶ Fine-tune lunar gravity assists, thrust arcs and eclipse reduction



Detailed Mission Plan

- ▶ Launch windows
- ▶ Contingency plans
- ▶ Other sub-system considerations



6.3 – JAXA's HITEN lunar mission

- ▶ Launched in Jan 1990 to highly elliptical Earth orbit (Uesugi 1988), HITEN was re-routed to the Moon but its propellant budget was insufficient for classical Hohmann or bielliptic transfer
- ▶ Variant of a novel class of trajectory (weak WSB) targeting Sun-Earth LP salvaged the mission (Belbruno and Miller 1993) by reducing transfer delta-V



Credit: https://space.skyrocket.de/img_sat/muses-a_1.jpg

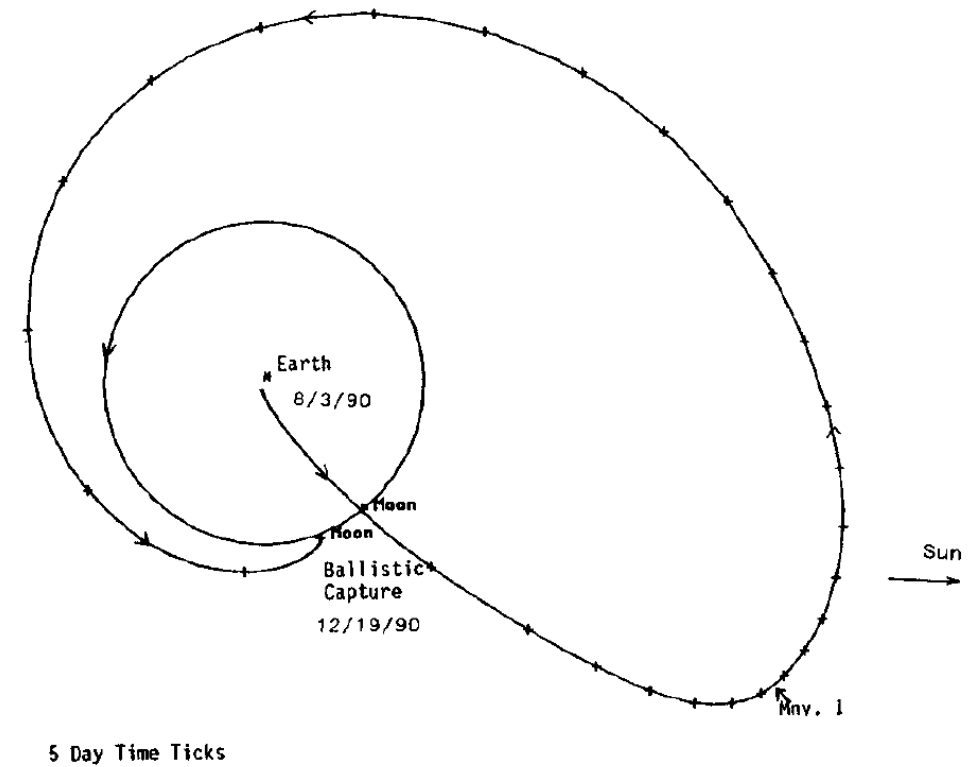


Figure 16: Numerical simulation of a ballistic capture transfer trajectory for the Japanese spacecraft Hiten: ecliptic plane projection, sun's direction indicated at Earth injection. (Belbruno and Miller 1993)

6.4 – Exterior Weak Stability Boundary Trajectories

- Since then, numerous works on various low-energy transfers have been performed, allowing for near ballistic lunar capture with reduced delta-V budget [low-energy \neq low-thrust]
 - ▷ Lunar orbit (Griesemer et al. 2011, Parker 2011)
 - ▷ NRHO (Parrish et al. 2020)

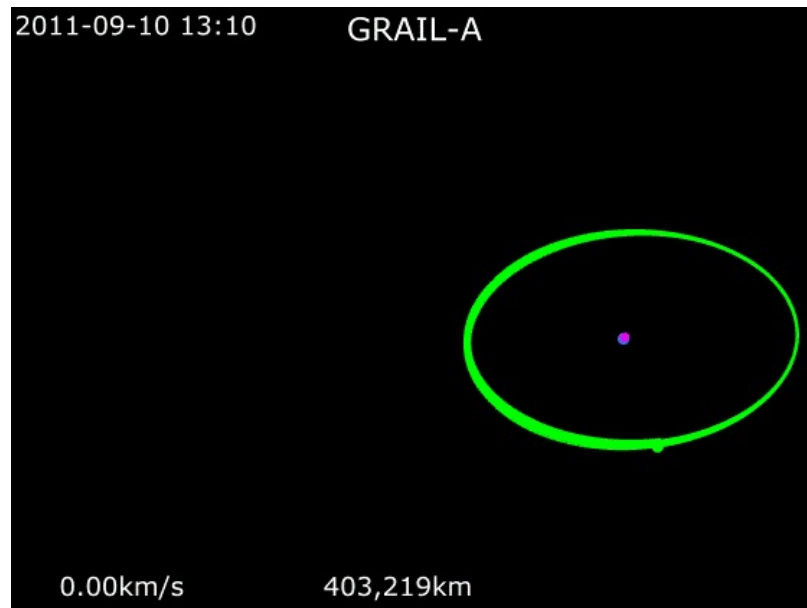


Figure 17: Trajectory of NASA's GRAIL spacecraft via exterior WSB. (Roncoli and Fujii 2010; Chung et al. 2010; Hatch et al. 2010)

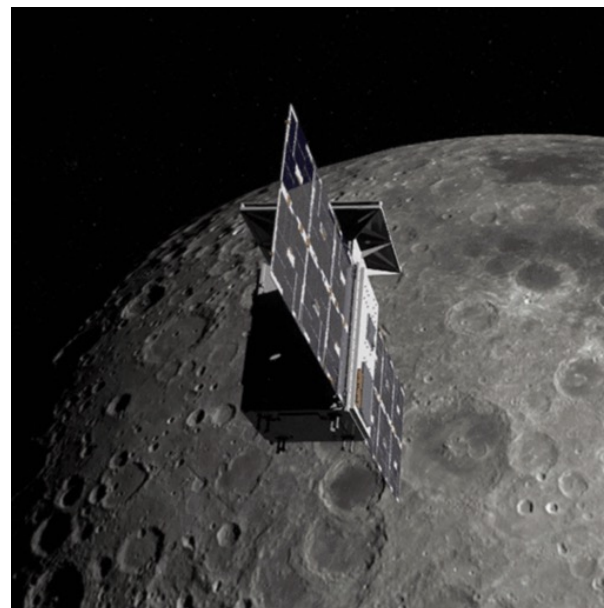


Figure 18: Artist impression of NASA's CAPSTONE, launching in 2021. (Parrish et al. 2020)

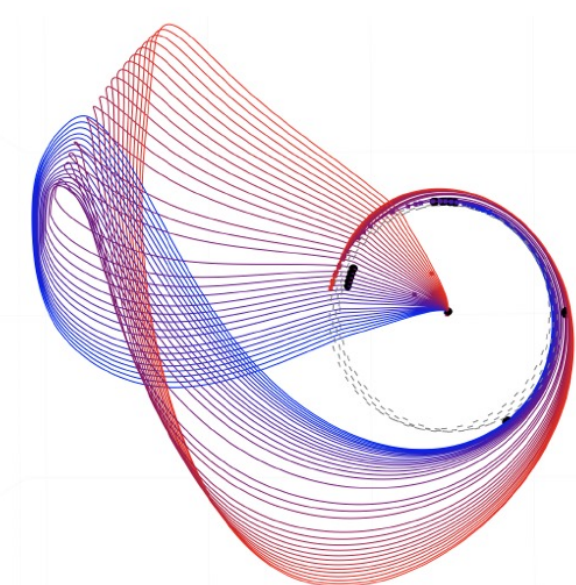


Figure 19: Family of BLT's to NRHO with outbound lunar flyby. (Dutt et al. 2018)

6.4 – Exterior Weak Stability Boundary Trajectories

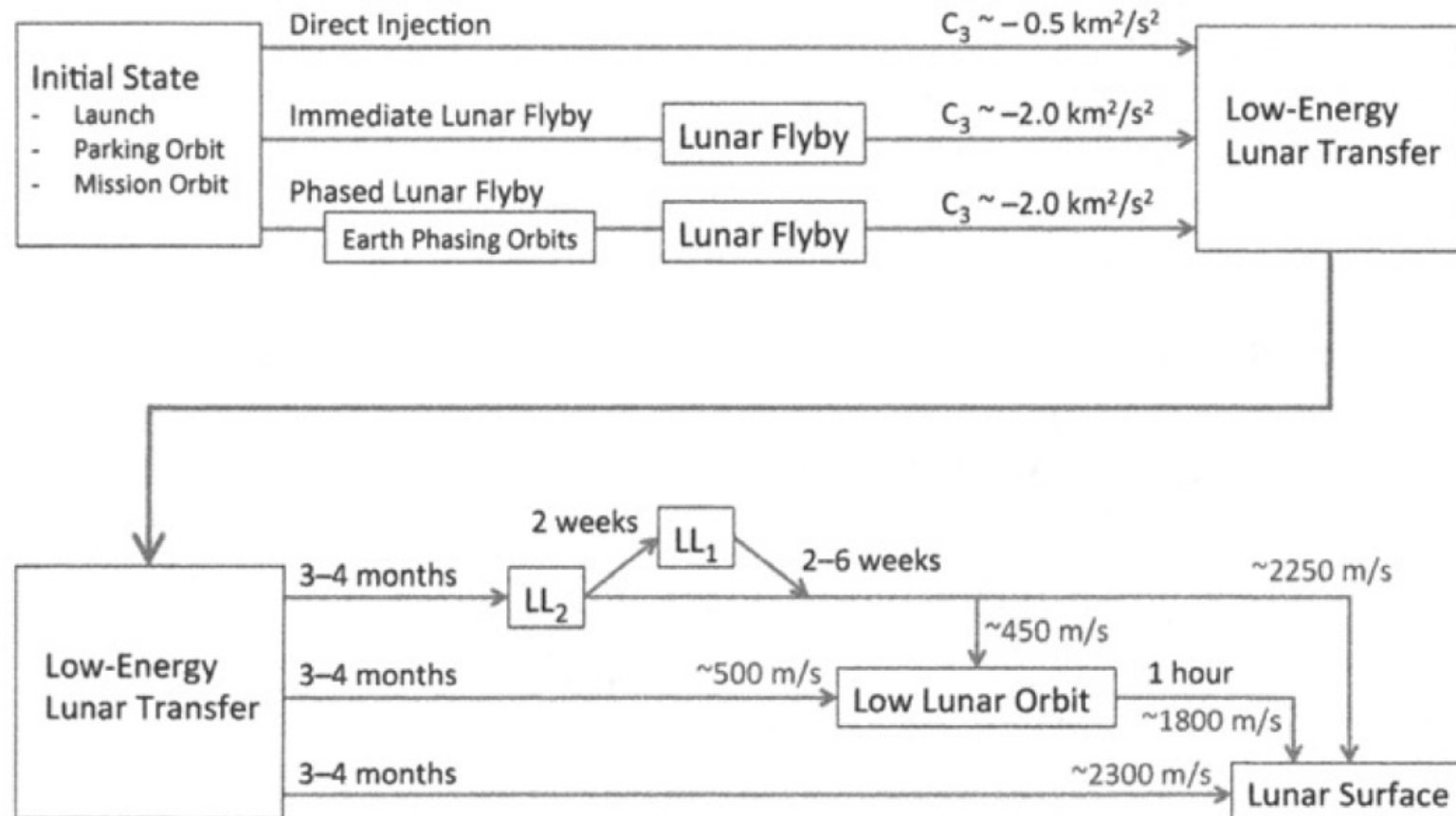


Figure 20: A flowchart illustrating different low-energy lunar transfer itineraries, with approximate C_3 values, transfer times and ΔV values shown (Parker et al. 2014)

6.4 – Exterior Weak Stability Boundary Trajectories

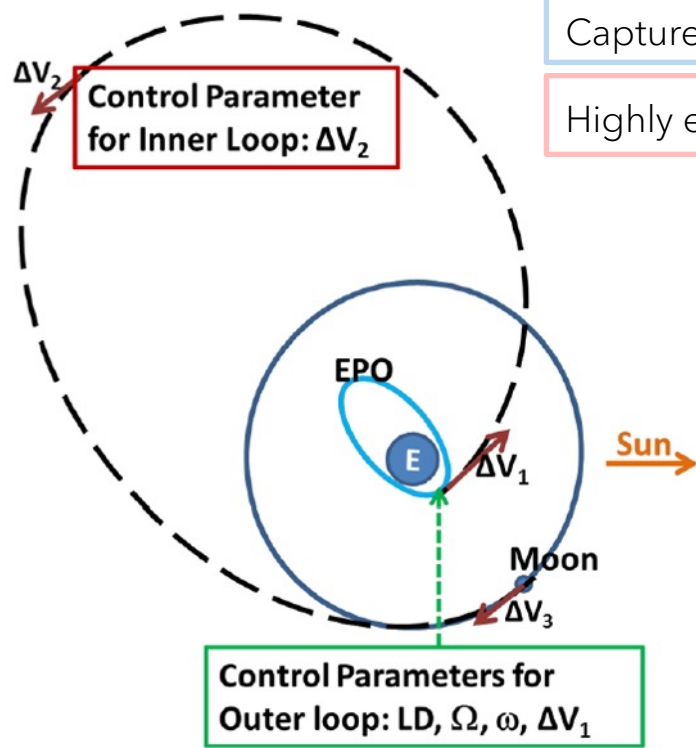


Figure 21: Control parameters for trajectory optimization – WSB moon. (Dutt et al. 2018)

EPO: 250 km x 23000 km, 18° inclination
LLO: 100 km altitude, circular

| Example 3 | | Example 4 | | | |
|--|------------------------------|-----------------------------|--|------------------------------|------------------------------|
| Event name | Direct | WSB | Event name | Direct | WSB |
| Launch date (UTC) | 10 Dec. 2017 19:26:40.000 | 9 Dec. 2017 23:04:58.000 | Launch date (UTC) | 19 Dec. 2017 23:14:12.626 | 19 Dec. 2017 23:04:58.000 |
| RAAN (deg) | 358.298 | 209.425 | RAAN (deg) | 120.181 | 353.693 |
| AOP (deg) | 66.731 | 348.803 | AOP (deg) | 42.170 | 51.953 |
| Time of flight (days) | 5 | 145.7 | Time of flight (days) | 5 | 119.5 |
| $\Delta V_{TLI}/\Delta V_1$ (km/s) | 0.973 | 1.0528 | $\Delta V_{TLI}/\Delta V_1$ (km/s) | 0.975 | 1.043 |
| Arrival periapsis altitude (km) | 1584.838 | 902019.761 | Arrival periapsis altitude (km) | 500 | 9706.958 |
| Arrival velocity magnitude (km/s) | 1.883 | 0.1007 | Arrival velocity magnitude (km/s) | 2.2648 | 0.270 |
| Arrival C3 (km^2/s^2) | 0.595 | -0.000098 | Arrival C3 (km^2/s^2) | 0.747 | -0.0001 |
| $\Delta V_{MOI}/\Delta V_2$ (km/s) | 0.7 | 0.0 | $\Delta V_{MOI}/\Delta V_2$ (km/s) | 0.8 | 0.000278 |
| Perilune altitude (km) | 1049.181 | 840028.570 | Perilune altitude (km) | 208.610 | 127550.758 |
| Apolune altitude (km) | 3525.088 | 8.68×10^6 | Apolune altitude (km) | 1544.415 | 168179.569 |
| Inclination (deg) | 8.950 | 94.959 | Inclination (deg) | 19.788 | 101.414 |
| Velocity (km/s) | 1.421 | 0.1007 | Velocity (km/s) | 1.778 | 0.165 |
| C3 energy (km^2/s^2) | -1.218 | -0.00103 | C3 energy (km^2/s^2) | -1.876 | -0.032772 |
| ΔV for 100 km circular orbit/ ΔV_3 (km/s) | 0.494 | 0.772 | ΔV for 100 km circular orbit/ ΔV_3 (km/s) | 0.237 | 0.835 |
| Total ΔV (km/s) | 2.167 | 1.825 | Total ΔV (km/s) | 2.012 | 1.878 |

Table 7: Test cases for WSB and direct transfer. (Dutt et al. 2018)

6.4 – Exterior Weak Stability Boundary Trajectories

- ▶ Low-energy transfers via Sun-Earth L_1 Lagrange point enabled by minimal mid-course correction Δv due primarily to the fortuitous coincidence in the energy levels of the Sun-Earth LPs and the Earth-Moon system (differing only about 50 m/s)
- ▶ Compared to traditional Hohmann transfer, mission fuel required is lowered by about 20%



6.5 – Kolmogorov-Arnold-Moser (KAM) Theory

- KAM theory addresses motions very close to those well-behaving and stable, whilst outside these regions, the motion is unstable and chaotic (entirely ballistic capture occurs here)

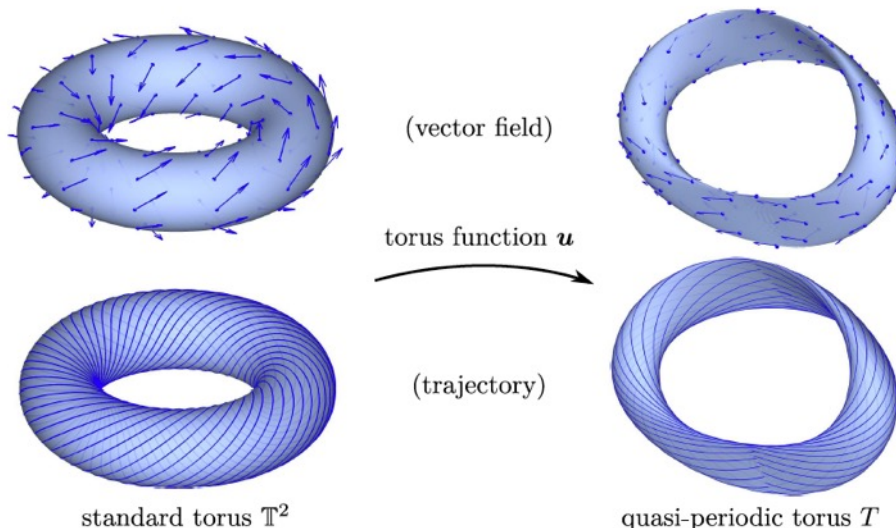


Figure 22: Left column – invariant tori with periodic orbits. Right column – quasi-periodic orbits^[27].

Invariant tori: each curve beginning on such torus starts and ends on its surface. Position of P on the torus can be defined with two angles, θ and ϕ

$$\theta = \omega_P \cdot t, \phi = \omega_2 \cdot t, f = \omega_P/\omega_2$$

- In CPR3BP, we have two primaries ($m_1 \gg m_2$) and massless body P moving in an elliptical motion around m_1 with orbital frequency ω_P . Reduction to basic two-body problem occurs by setting $\mu_2 = Gm_2 = 0$.
- Using a rotating coordinate frame centered at m_1 (m_2 fixed), one will observe P moving on an ellipse that precesses with frequency ω_2 , which is also the orbital frequency of m_2 around the barycenter. P traces out a 2D torus.

- If f is rational, motion of P is periodic and curve on torus is closed.
- Else, P will move densely on the torus and never return to its starting point.
- Varying semi-major axis and frequency ω_P generates different invariant tori, inside one another, creating a 3D energy manifold.

6.5 – Kolmogorov-Arnold-Moser (KAM) Theory

- From the Jacobi integral C , we have (ε_0 = energy of P, h_P = angular momentum of P):

$$\varepsilon_0 = \overrightarrow{\omega_2} \cdot \overrightarrow{h_P} - \frac{C_J}{2}$$

- In R3BP, C is the only conserved quantity. In 2BP, ε_0 and h_P are conserved too.

- KAM describes what happens to the invariant tori when $\mu_2 \neq 0$

- Energy of P re-expressed, $F(\mathbf{r})$ is the perturbation function in the rotating frame:

$$\varepsilon = \varepsilon_0 + \epsilon \cdot F(\mathbf{r})$$

$$\epsilon = \frac{\mu_2}{\mu_1}$$

- KAM states that if ϵ is sufficiently small, most irrational invariant tori do not vanish, although

the rational ones do

- Gaps, whose size are somewhat proportional to the value of ϵ , will appear between irrational invariant tori, where rational invariant tori used to exist

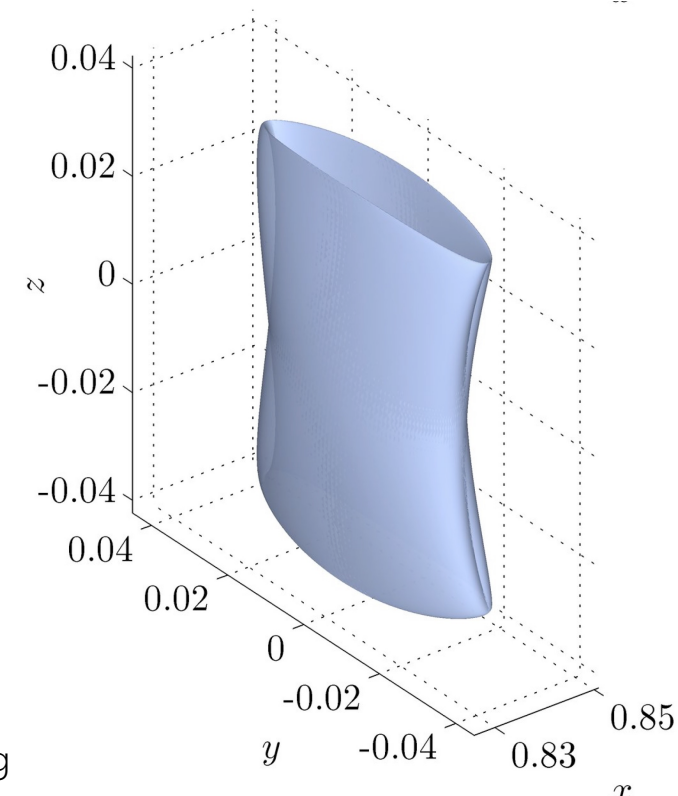


Figure 23: Family of Earth-Moon Lissajous tori.
(Olikara 2010)

6.5 – Kolmogorov-Arnold-Moser (KAM) Theory

- ▶ Resultant behavior:
 - ▷ Outside gaps (irrational tori): motion is stable and precessing ellipses persist
 - ▷ Within gaps (used to be rational tori): motion is chaotic
- ▶ Each 2D torus gap divides the 3D energy manifold (in strictly 3BP) into two non-communicating parts
- ▶ In n -BP, a higher dimensional torus will allow certain irrational tori to connect through the gaps, allowing a particle to 'leak out' (phenomenon known as Arnold's diffusion) and reach other energy manifolds
- ▶ Explanation for the Kirkwood gaps in the Jovian asteroid belt

6.5 – Kolmogorov-Arnold-Moser (KAM) Theory

- ▶ Study of the Sun-Jupiter + asteroid 12 Victoria system (Celletti et al. [2005](#))
- ▶ Low-energy capture of asteroids onto KAM tori (Verrier and Collin [2015](#))
- ▶ Computation of Quasi-periodic tori in Earth-moon CR3BP (Olikara [2010](#))

6.6 – Conclusion

- ▶ Demonstrated low-thrust ballistic lunar transfer trajectory
- ▶ Introduced low-energy exterior Weak Stability Boundary lunar transfers that require high thrust propulsion with lower delta-v trade-off

7.1 – Bibliography

- Araujo, R. A. N., Winter, O. C., Prado, A. F. B. A., & Vieira Martins, R. (2008). Sphere of influence and gravitational capture radius: a dynamical approach. *Monthly Notices of the Royal Astronomical Society*, 391(2), 675-684.
- Arenstorf, R. F. (1963). Periodic solutions of the restricted three body problem representing analytic continuations of Keplerian elliptic motions. *National Aeronautics and Space Administration*.
- Belbruno, E. (1987). Lunar capture orbits, a method of constructing earth moon trajectories and the lunar GAS mission. In 19th International Electric Propulsion Conference (p. 1054).
- Belbruno, E. A., & Miller, J. K. (1993). Sun-perturbed Earth-to-Moon transfers with ballistic capture. *Journal of Guidance, Control, and Dynamics*, 16(4), 770-775.
- Bodin, P., Berge, S., Bjork, M., Edfors, A., Kugelberg, J., & Rathsman, P. (2004). The SMART-1 attitude and orbit control system: Flight results from the first mission phase. In AIAA Guidance, Navigation, and Control Conference and Exhibit (p. 5244).
- Celletti, A., & Chierchia, L. (2005). KAM stability for a three-body problem of the solar system. *Zeitschrift für angewandte Mathematik und Physik ZAMP*, 57(1), 33-41.
- Conley, C. C. (1968). Low energy transit orbits in the restricted three-body problems. *SIAM Journal on Applied Mathematics*, 16(4), 732-746.
- Curtis, H. D. (2013). Orbital mechanics for engineering students. Butterworth-Heinemann.
- Di Cara, D. M., & Estublier, D. (2005). Smart-1: An analysis of flight data. *Acta Astronautica*, 57(2-8), 250-256.
- Dutt, P., Anilkumar, A. K., & George, R. K. (2018). Design and analysis of Weak Stability Boundary trajectories to Moon. *Astrophysics and Space Science*, 363(8), 1-10.
- Epenoy, R., & Pérez-Palau, D. (2019). Lyapunov-based low-energy low-thrust transfers to the Moon. *Acta Astronautica*, 162, 87-97.
- Fesenkov, V. G. (1946). On the possibility of capture at close passages of attracting bodies. *Astronomicheskiy zhurnal*, 23(1), 45-48.
- Griesemer, P. R., Ocampo, C., & Cooley, D. S. (2011). Targeting ballistic lunar capture trajectories using periodic orbits. *Journal of guidance, control, and dynamics*, 34(3), 893-902.

7.1 – Bibliography

- Kluever, C. A., & Pierson, B. L. (1995). Optimal low-thrust three-dimensional earth-moon trajectories. *Journal of Guidance, Control, and Dynamics*, 18(4), 830-837.
- Koon, W. S., Lo, M. W., Marsden, J. E., & Ross, S. D. (2000). Dynamical systems, the three-body problem and space mission design. In *Equadiff 99: (In 2 Volumes)* (pp. 1167-1181).
- Olikara, Z. P. (2010). Computation of quasi-periodic tori in the circular restricted three-body problem (Doctoral dissertation, Purdue University).
- Parker, J. S. (2011). Targeting low-energy ballistic lunar transfers. *The Journal of the Astronautical Sciences*, 58(3), 311-334.
- Parker, J. S. (2011). Targeting low-energy ballistic lunar transfers. *The Journal of the Astronautical Sciences*, 58(3), 311-334.
- Parker, J. S., & Anderson, R. L. (2014). *Low-energy lunar trajectory design* (Vol. 12). John Wiley & Sons.
- Parrish, N. L., Kayser, E., Udupa, S., Parker, J. S., Cheetham, B. W., & Davis, D. C. (2020). Ballistic Lunar Transfers to Near Rectilinear Halo Orbit: Operational Considerations. In *AIAA Scitech 2020 Forum* (p. 1466).
- Racca, G. D. (2003). New challenges to trajectory design by the use of electric propulsion and other new means of wandering in the solar system. *Celestial Mechanics and Dynamical Astronomy*, 85(1), 1-24.
- Rathsman, P., Kugelberg, J., Bodin, P., Racca, G. D., Foing, B., & Stagnaro, L. (2005). SMART-1: Development and lessons learnt. *Acta Astronautica*, 57(2-8), 455-468.
- Uesugi, K., Hayashi, T., & Matsuo, H. (1988). MUSES-A double lunar swingby mission. *Acta Astronautica*, 17(5), 495-501.
- Vasile, M., Bernelli-Zazzera, F., Fornasari, N., & Masarati, P. (2002). Design of interplanetary and lunar missions combining low thrust and gravity assists. final report of esa/esoc study contract, 14126(00).
- Verrier, P. E., & McInnes, C. R. (2015). Low-energy capture of asteroids onto kolmogorov–arnold–moser tori. *Journal of Guidance, Control, and Dynamics*, 38(2), 330-335.

End